Catena 235 (2024) 107621

Contents lists available at ScienceDirect

Catena

journal homepage: www.elsevier.com/locate/catena

# Geochemistry and mineralogy of muds and thermal waters from mud volcanoes in the NW Caribbean Coast of Colombia and their potential for pelotherapy

Maurizio Palmisano [a], Giuseppina Balassone [b,c], Sabino Maggi [d,e,*], Alexander Armesto Arenas [f], Iber M. Banda Guerra [g], Luis E. Correa Valero [g], Feliciano Ippolito [h], Nicola Mondillo [b,i], David F. Morales Giraldo [g], Angela Mormone [c], Annamaria Pellino [b], Francesco Putzolu [i], Diana Di Luccio [j]

[a] Institute for Agricultural and Forest Systems in the Mediterranean CNR-ISAFOM, National Research Council, 82100 Benevento, Italy
[b] Department of Earth, Environment and Resources Sciences, University of Naples Federico II, 80126 Naples, Italy
[c] Vesuvian Observatory, National Institute of Geophysics and Volcanology, 80124 Naples, Italy
[d] Institute of Atmospheric Pollution Research CNR-IIA, National Research Council, 70125 Bari, Italy
[e] Faculty of Engineering, International Telematic University UniNettuno, 00186 Rome, Italy
[f] Department of Agricultural and Environmental Sciences, University Francisco de Paula Santander, 546552 Ocaña, Norte de Santander, Colombia
[g] Instituto de Investigaciones Marinas y Costeras INVEMAR, Santa Marta, Colombia
[h] Department of Agricultural, Environmental and Food Sciences, University of Molise, 86100 Campobasso, Italy
[i] Natural History Museum, SW7 5BD London, UK
[j] Department of Science and Technologies, University of Naples Parthenope, 80138 Naples, Italy

ARTICLE INFO

*Keywords:*
Mud volcanoes
Thermal mud and waters
Grain size
Mineralogy
Geochemistry
Pelotherapy

ABSTRACT

Mud volcanoes in northwestern Colombia are used by local people as inexpensive recreation and wellness centres, especially for pelotherapy. However, the potential therapeutic value of the muds and thermal waters released by these volcanoes has not been fully investigated. The main objective of this research is to determine the potential therapeutic value of the solid and liquid fractions of the muds sampled from nine mud volcanoes located along the northwestern Caribbean coast of Colombia through geochemical and mineralogical analysis. An evaluation of the granulometric characteristics was also carried out. The presence of a hypertonic saline environment created by secondary volcanic processes is indicated by the thermal fluid fraction. The mineral composition of the muds is dominated by quartz, phyllosilicates (kaolinite, smectite, illite and chlorite), feldspar, carbonates (dolomite, calcite) and a significant amorphous component. Based on the composition of the clay fraction, three distinct groups can be distinguished: (i) kaolinite-rich, (ii) illite-rich, and (iii) chlorite-rich. These muds are suitable for use by the local population due to the extremely low levels of contaminants harmful to human health, such as potentially toxic elements, nitrates, nitrites or fluorides. The results of this study suggest that the muds and thermal waters released by these mud volcanoes have potential therapeutic value. Further research is needed to confirm these findings and to investigate the specific mechanisms by which these muds and waters can be used in medical practice.

## 1. Introduction

Mud volcanoes (MVs), also known as diapirs, are widespread worldwide and occur in a wide range of geodynamic settings. Mud volcanoes usually appear as cone-shaped structures ranging in height from a few centimeters to hundreds of meters and with variable aspect

* Corresponding author at: Institute of Atmospheric Pollution Research CNR-IIA, National Research Council, 70125 Bari, Italy.
*E-mail addresses:* maurizio.palmisano@cnr.it (M. Palmisano), balasson@unina.it (G. Balassone), sabino.maggi@cnr.it (S. Maggi), aarmestoa@ufpso.edu.co (A.A. Arenas), f.ippolito93@libero.it (F. Ippolito), nicola.mondillo@unina.it (N. Mondillo), david.morales@invemar.org.co (D.F. Morales Giraldo), angela.mormone@ingv.it (A. Mormone), annamaria.pellino@unina.it (A. Pellino), francesco.putzolu1@nhm.ac.uk (F. Putzolu), diana.diluccio@uniparthenope.it (D. Di Luccio).

https://doi.org/10.1016/j.catena.2023.107621
Received 7 June 2023; Received in revised form 6 October 2023; Accepted 20 October 2023
Available online 3 November 2023

ratios. In most cases, they have a single crater at the summit, but it is not uncommon for MVs to have multiple vents of different shape and size (Higgins and Saunders, 1974; Carvajal et al., 2011). Mud volcanoes are still poorly understood geological structures (Panzera et al., 2016; Maestrelli et al., 2019). Their eruptions are characterized by moderate temperatures, rarely exceeding 30°C (Mazzini and Etiope, 2017) and are usually composed of a solid inorganic fraction, consisting mainly of fine-grained sediments, as well as of an organic component that includes microflora, microfauna, humus and other humo-mineral compounds mixed with a thermal liquid phase and a gaseous phase. Periods of dormancy are interspersed with eruptive phases during which these mixtures are extruded through preferential pathways, such as fractures or vents (Dill and Kaufhold, 2018).

There are currently a few thousand known onshore mud volcanoes (Fig. 1), while the number of those laying on the seafloor is unknown (Kopf, 2002; Baloglanov et al., 2018). Subaqueous MVs often occur at convergent margins, where oceanic sediments are transported towards the subduction trench following the plate kinematics. These areas of tectonic compression can be characterized by thick sedimentary sequences that are rapidly deposited near and within the trench.

The Atlantic Ocean contains hundreds of onshore and offshore mud volcanoes but the vast majority of them can be found along the Caribbean thrust belt. Most of the nearly 110 active terrestrial Caribbean MVs are located in northern Colombia, north-eastern Venezuela, Trinidad (Dimitrov, 2002; Hosein et al., 2014) or in the Barbados accretionary complex (Brown and Westbrook, 1988; Deville et al., 2003).

The northwestern part of Colombia has a large number of mud volcanoes, mostly located along the Sinú-San Jacinto fold belt, at the convergence between the Caribbean plate and the northwestern margin of the South American plate (Di Luccio et al., 2021). Sedimentary volcanism in this area is also associated with soil erosion and desertification and is favored by the fluvial sediment input from the Rio Magdalena (Atencio and Mendoza, 2018). The typical alkaline environment of the MVs, characterized by the presence of basic soils and high salinity levels, also influences the local vegetation, as only a few tolerant species can survive in this extreme environment (Ren et al., 2018; Sokol et al., 2019).

In some cases, these geological structures have become tourist attractions (such as the El Totumo mud volcano in Santa Catalina, Bolívar Department or the Virgen del Cobre Necoclí mud volcano in Antioquia department, the largest mud volcano in Colombia with a 10 m wide mouth.) and have promoted the creation of a network of small "tourist-therapeutic" local businesses that take advantage of the large amount of mud available.

Research on mud volcanoes has usually focused on their relationship with hydrocarbon reservoirs (Conti et al., 2014), or possible relationships with the local seismicity (Etiope et al., 2004; Mazzini and Etiope, 2017). In a recent work, Di Luccio et al. (2021) presented the first multi-analytical study of MVs located in the northwestern area of the Colombian Caribbean coast, mainly focusing mainly on the characterization of the chemical and isotopic nature of the gaseous and liquid phases as well as the evaluation of the vulnerability index associated with the MVs. They also carried out a preliminary study of the solid fraction of the muds using quantitative X-ray powder diffraction, to determine the amounts of clay minerals, carbonates and quartz present in the samples.

This paper presents a new multidisciplinary study conducted on samples collected in mid-2021 from the same MVs as those studied in the previous work (Di Luccio et al., 2021). Here, we report further chemical analyses of the aqueous phase, as well as new granulometric, geochemical, and mineralogical analyses on the solid fraction (sediments). Indeed, a better understanding of the nature of the sediments and thermal waters can potentially help to define the fields of application and therapeutic uses of MVs from the Caribbean area.

### 1.1. Origin and therapeutic uses of pelotherapy

Clay minerals are present in significant amounts in various geomaterials, and their solubilization by thermal water allows for their extraction and subsequent utilization in medicine, pharmacology, cosmetics, and spa treatments (Galzigna et al., 1995; Jobstraibizer, 1999; Carretero, 2002; Veniale et al., 2004; Gomes, 2005; Gomes and Silva, 2006; Veniale et al., 2007; Photos-Jones et al., 2016; Gomes et al., 2021).

Thermal water has always been considered the simplest and most natural medical treatment. The earliest evidence of its use for therapeutic purposes can be found in some Sumerian tablets, which clearly mention the use of water in medicine (Sánchez-Espejo et al., 2014). Furthermore, the use of thermal mud for therapeutic purposes dates back to the Sumerian era, and later to the Egyptian Empire. Thanks to

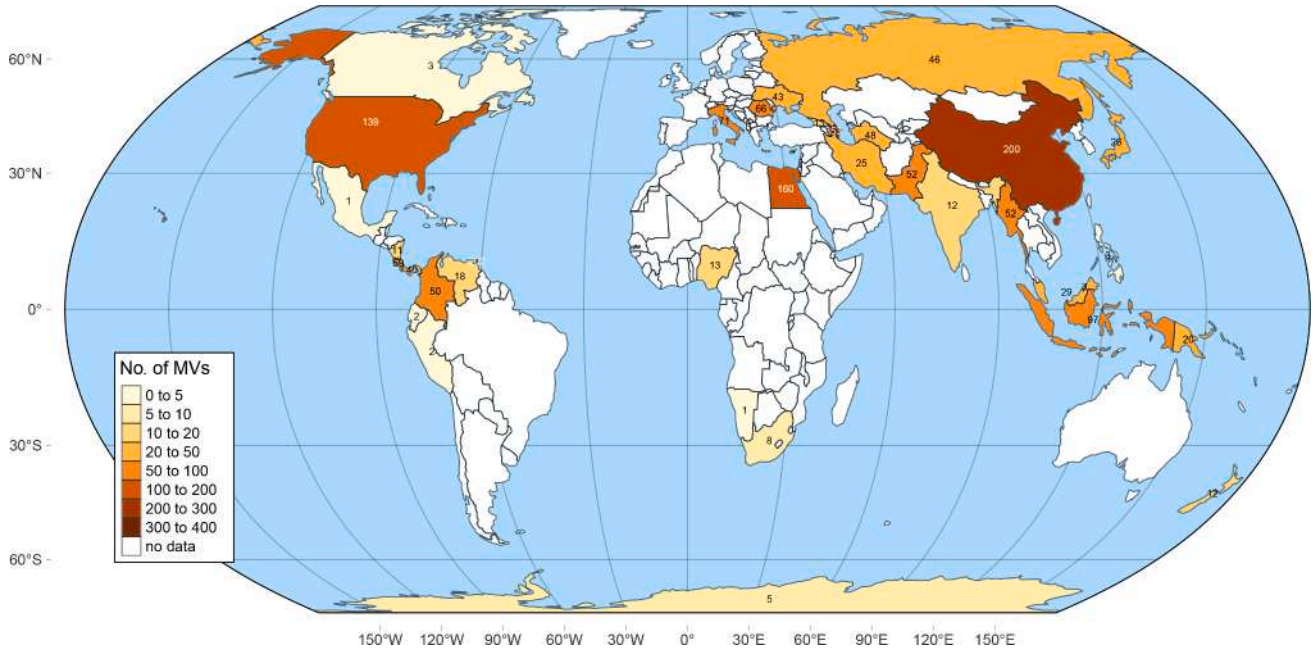


**Fig. 1.** World distribution of onshore mud volcanoes (data from Baloglanov et al. (2018)). The number of identified MVs is overlaid on each country.

Hippocrates, the Hellenic era saw the first specific references to the medical use of thermal mud, which was resumed and applied on a larger scale throughout the Roman Empire (Carretero, 2002). During the Middle Ages, interest in thermal treatments and frequentation of baths declined almost completely, probably due to changes in habits and traditions brought about by the rise of Christianity (Carretero et al., 2006). The Renaissance brought a renewed interest in thermal baths, prompted by the work of several prominent doctors, such as Ugolino da Montecatini, Antonio Benivieni, and Jean François Fernel (Danzi, 2017). This renewed interest continued throughout the pre-industrial era thanks to the contribution of doctors and scientists who pioneered the first scientific studies on thalassotherapy and hydrotherapy. At the beginning of the nineteenth century hydrotherapy was officially included as a subject of study in the Faculty of Medicine in Vienna (Jobstraibizer, 1999). Today, with more than 400 active spas distributed throughout its territory, Italy is recognized as the home of thermal treatments. Many of these structures date back to the Roman age and are still the preferred destination of a tourism dedicated to psycho-physical well-being (Veniale et al., 2004; Veniale et al., 2007).

The first attempt to standardize the use of mud for medical purposes dates back to the late 1940s. During the *IVème Conférence Scientifique Internationale* held in Dax, France, at the end of 1949, the General Assembly of the International Society of Medical Hydrology (ISMH) defined the essential parameters for classifying muds according to their origin, chemical composition, temperature and maturation conditions, as well as their geological, chemical, and physical characteristics (Burt, 1949). During the same Conference, the ISMH also coined the definition of *peloid*, indicating with this term all natural or artificial mixtures consisting of thermo-mineral water containing organic and/or inorganic materials used for therapeutic purposes. A typical example of peloids is thermal mud. *Pelotherapy* is therefore the external application of peloids for therapeutic and skin care purposes, which are usually applied in baths with water of various compositions at temperatures close to 45 −50°C. The therapeutic effect of peloids may be due to thermal treatment, the chemistry of the salt water and the properties of the clay.

In 2004, Lüttig (2004) proposed another classification of peloids, based on geological parameters. However, this classification is rather complex, especially with regard to their nomenclature. More recently, Gomes et al. (2013) introduced a new definition and classification of peloids, taking into account their origin, composition, and applications.

These two works broadly define a peloid as a mature mud or a mature mud dispersion having therapeutic or cosmetic properties, composed of a complex mixture of mineral or sea water, natural fine-grained materials of geological or biological origin, and organic compounds derived from biological metabolic activity.

The therapeutic properties of thermal muds are related to several factors, including granulometry, which is particularly important because the cationic exchange between the mineral phases and the skin is strongly dependent on grain size. In general, smaller grain sizes in the solid fraction of thermal mud result in higher exchange capacity and reactivity (Carretero et al., 2007; Quintela et al., 2012; Gomes et al., 2013). In addition, the contact surface area and thus the adhesion of the mud to the skin is strongly influenced by the grain size. The presence of water in clay lattices further increases adhesiveness, allowing clays to adhere more easily to the surfaces to which they are applied and release their active components (Rebelo et al., 2015). However, not all clay minerals exhibit the same level of adhesiveness (Pozo et al., 2019). Smectite, in particular, is characterised by a very high capacity to retain water within its interlayers, and thus by a high level of adhesiveness. Therefore, a thermal mud composed mainly of smectite will have a greater and more effective therapeutic activity, precisely because it will adhere better and for a longer time to the skin, allowing a prolonged release of the active components contained in the mud. Wet clays also become smooth and slippery.

### 1.2. Mud maturation process

The maturation process of the clays plays a key role in defining the therapeutic properties of the resulting thermal muds. This process can be natural and can take place *on-site*, i.e., in the same source basin of the muds, or induced *off-site*, using special tanks where the clay is immersed in thermal water or is subjected to a continuous and constant flow of thermal water (Tateo and Summa, 2007; Veniale et al., 2004).

The natural on-site maturation process is a slow and complex process that takes place in a natural thermal "pool", without any human intervention. The process is driven by a combination of factors, including heat, which accelerates the chemical reactions that lead to the formation of new clay minerals, and water, which acts as a solvent and a catalyst and also helps to transport dissolved minerals. The composition of the dissolved minerals in the thermal pool water also plays a key role in determining the type and properties of the clay minerals that form.

Off-site maturation consists of extracting clay from the bottom of the thermal pools and, after filtration, placing it in special tanks. In these tanks, the clay is immersed in thermal water, kept at a constant temperature and exposed to the action of sunlight. The thermal water, with its temperature and chemical composition, has a great influence on the resulting thermal mud by promoting the development of microflora and allowing it to mature. Off-site maturation can last from several months to a year. The final chemical, physical and mineralogical characteristics acquired by the thermal muds will depend on the specific technique used to bring them into contact with the thermal water.

In the case of the muds from the nine volcanoes studied here, the entire maturation process occurs naturally because the clay sediments are permanently immersed in natural pools of thermal water. This condition favors the continuous exchange of organic and inorganic compounds, modifying the original composition of the peloids.

The chemistry of the thermal water and its temperature play a primary role in the therapeutic potential of the mud (Quintela et al., 2015; Rebelo et al., 2015). In addition to altering the chemical and physical characteristics of the clays, the maturation process leads to the development of a complex community of non-pathogenic microorganisms composed of bacteria, algae, diatoms, protozoa, microfauna and humus, which make up the organic component of the clays (Gomes and Silva, 2007). These microorganisms, by releasing organic compounds with their metabolic activity, enhance the therapeutic effects of the thermal peloid (Carretero, 2020; Cara et al., 2000; Fernández-González et al., 2013). Sunlight also plays an important role in the maturation process: when the tanks are exposed to the sun, significant variations in the physico-chemical parameters of the mature are observed compared to the original intact mud, and these variations strongly affect the final therapeutic properties of the peloids (Aguzzi et al., 2013; Armijo et al., 2016).

It should be noted that the analysis of the microorganisms present in the thermal muds and their potential pathogenicity falls outside the scope of the current work, which focuses on the geochemical and mineralogical characteristics of the muds emitted by the MVs studied here.

## 2. Study area

The study area is located in the northwestern part of Colombia, between the cities of Barranquilla in the northeast and Cartagena in the southwest, (Fig. 2), and is characterized by a conspicuous number of diapiric structures located along the Sinú-San Jacinto fold belt (Aristizábal et al., 2009), an active accretionary prism formed by the convergence between the Caribbean plate and the northwestern margin of the South American plate (Dill et al., 2022; García-Delgado et al., 2022). This convergence process, which is still ongoing, began in the early Cenozoic and led to the development of southeast-oriented compressive stresses. It is precisely on the Sinú-San Jacinto belt that most of the active Colombian MVs, such as those studied in this work,

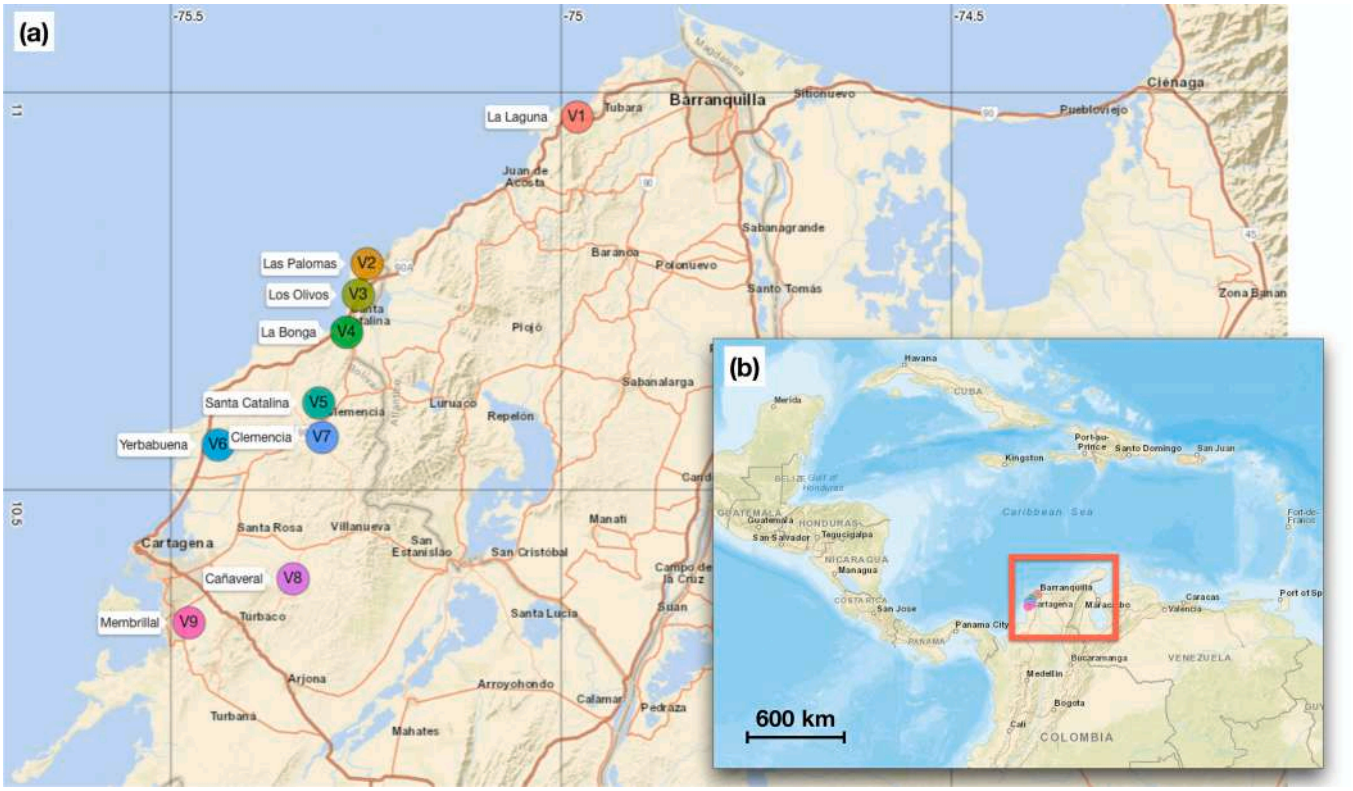


**Fig. 2.** (a) Map of the study area, showing the locations of the 9 MVs considered in this work: La Laguna (V1), Las Palomas (V2), Los Olivos (V3), La Bonga (V4), Santa Catalina (V5), Yerbabuena (V6), Clemencia (V7), Cañaveral (V8), and Membrilla (V9). (b) Location of the study area within the broader Caribbean region. Further details of the study area can be found in (Di Luccio et al., 2021).

are located.

The lower outcropping units are Late Paleocene to Early Eocene lithic arenites interbedded with muds and conglomerates. Above these units are Miocene arenites. These units, like the others consisting of marls and argillites, contain amounts of glauconite, which is a proxy of a marine depositional environment (Vernette et al., 1992; Cediel et al., 2003; Mantilla-Pimiento et al., 2009; Vinnels et al., 2010). The upper units of the sedimentary sequence (Late Miocene), are deposited in conformity with the layers below. Holocene sediments, originating from primordial marshes, are widely present along the entire coastal area. These sediments are composed mainly of organic matter deposited in the Magdalena River system.

The mud volcanoes located in the study area (Fig. 3 and Table 1) have features in common with other mud volcanoes occurring in a similar tectonic and sedimentary context, being characterized by strong seismicity accompanied by frequent eruptions of large amounts of solid and liquid mixtures (Dimitrov, 2002; Mazzini and Etiope, 2017). During the sampling campaign, no secondary volcanic manifestations, such as fumaroles, sulfataras, geysers, boriferous heads and *putizze*, associated with the mud volcanoes were observed in the vicinity of our study area.

The eruptive processes of MVs are due to the formation of highly compressed clay flows that can rise up to the surface through fractures and fault zones, vents or other areas of weakness. Once erupted, these clayey flows give rise to the formation of conical structures whose sides assume a more or less steep inclination according to the plasticity of the main clay species (Carvajal et al., 2011; Carvajal and Mendivelso, 2011; Dill and Kaufhold, 2018). Therefore, the analysis of the mineralogical composition as well as of the physico-chemical parameters of the peloids erupted from the MVs provides useful information about the studied area and the mechanisms that led to the formation of its environment.

As already noted in Di Luccio et al. (2021), these Colombian MVs are often considered landscape and tourist attractions as well as a therapeutic resource (Fig. 4). However, they also represent a risk to local communities, due to the frequent and unexpected, eruptions, often accompanied by the release of toxic gases or by landslides, that can damage the infrastructure and can pose a threat to the local population.

## 3. Materials and methods

Clay and water samples were collected from nine MVs located along the northwestern Colombian Caribbean coast during a sampling campaign conducted in mid-2021. The MVs are located in the departments of Atlantico (La Laguna MV), Bolivar (Las Palomas, La Bonga, Santa Catalina, Yerbabuena, Clemencia and Membrillal MVs), Cordoba (Los Olivos MV) and Magdalena (Cañaveral MV) (Fig. 2 and Table 1).

For each MV, 2 samples for the liquid fraction and 2 samples for the solid fraction were collected. Sampling was carried out using polyethylene or PTFE tools and sample holders to avoid contact with metal components, which might pose a risk of contaminating the collected samples.

The liquid phase was sampled using a 100 ml Falc syringe attached to the end of a silicone tubing positioned near the center of the volcanic cone. The clay sediments were sampled from the center of each emission zone at a depth of approximately 50 cm below the ground surface (Fig. 3). To prevent thermal modification of the clay lattices, the samples were dried in an oven at 40°C for three days, keeping the temperature stable within ±1°C.

### 3.1. Granulometric and geochemical analysis

Prior to grain size analysis, the samples were powdered by grinding in a corundum mill, using acetone as a lubricant, and subjected to quartering to obtain at least two representative fractions.

The collected fractions were treated in a 1 : 10 solution consisting of 10 ml of 15% $H_2O_2$ (hydrogen peroxide) in 100 ml of distilled water, to remove all salt content and part of the organic material present in the


**Fig. 3.** Images of the MVs during the sampling operations, showing either the main eruptive center or the bubbling vents: (a) La Laguna (V1), (b) Las Palomas (V2), (c) Los Olivos (V3), (d) La Bonga (V4), (e) Santa Catalina (V5), (f) Yerbabuena (V6), (g) Clemencia (V7), (h) Cañaveral (V8) and (i) Membrillal (V9).

**Table 1**
Location of the sampled mud volcanoes in northwestern Colombia. Geographic coordinates are in the WGS84 system. More information on these MVs can be found in Di Luccio et al. (2021).

| MV | Site name | Department | Latitude (N) | Longitude (W) |
|---|---|---|---|---|
| V1 | La Laguna | Atlántico | 10°58′08.70″ | −74°58′41.94″ |
| V2 | Las Palomas | Bolívar | 10°47′05.58″ | −75°14′51.06″ |
| V3 | Los Olivos | Cordóba | 10°44′42.36″ | −75°15′33.12″ |
| V4 | La Bonga | Bolívar | 10°41′56.40″ | −75°16′26.40″ |
| V5 | Santa Catalina | Bolívar | 10°36′32.40″ | −75°18′36.00″ |
| V6 | Yerbabuena | Bolívar | 10°33′21.60″ | −75°26′20.40″ |
| V7 | Clemencia | Bolívar | 10°33′58.02″ | −75°18′22.68″ |
| V8 | Cañaveral | Bolívar | 10°23′14.22″ | −75°20′36.48″ |
| V9 | Membrillal | Bolívar | 10°19′57.24″ | −75°28′35.04″ |

samples. The carbonate fraction was removed by chemical etching with HCl prior to sieving. After this pretreatment, the samples were sieved at 63 $\mu$m, which is conventionally considered the lower size limit for sand. The whole operation was performed under wet conditions (Krumbein, 1934).

To preserve the integrity of the sample and its mineralogical components, the collected samples were air-dried and then gently ground in an agate mortar using acetone as a lubricant.

Particle size analysis of the samples was performed using a Malvern Panalytical Mastersizer 3000 laser diffraction particle size analyzer, capable of measuring the particle size and particle size distribution from 0.01 $\mu$m to 3.5 mm.

**Fig. 4.** Therapeutic bath in the Yerbabuena mud volcano, taking advantage of the potential health benefits of the mineral-rich mud.

To analyze the metals present in the sediments, hot acid extraction

was performed using a solution of $HNO_3$ and $H_2O_2$ followed by centrifugation, and the resulting mixture was analyzed by inductively coupled plasma optical emission spectroscopy (ICP-OES) using a ThermoFisher iCAP PRO ICP-OES.

The water samples were collected using a vacuum filtration system to avoid contact between the aqueous phase and the potentially polluting solid fractions. The main physical and chemical parameters of the samples, namely temperature T, pH, electrical conductivity EC, and oxidation–reduction potential Eh, were measured using an YSI EXO1 portable multi-parameter probe.

The anion content of the aqueous samples ($Cl^-$, $SO_4^{2-}$, $NO_2^-$, $NO_3^-$) was determined using a ThermoFisher Dionex Aquion ion chromatography system.

### 3.2. Mineralogical analysis

Micromorphological, textural and qualitative chemical analyses of the mineralogical components of the muds were performed by scanning electron microscopy with energy dispersive X-ray spectroscopy (SEM-EDS) using a JEOL JSM 5310 instrument equipped with an Oxford Energy Dispersive Spectrometry (EDS) INCA X-stream pulse processor and ETAS INCA (Integrated Calibration and Application Tool) software, version 4.08. The SEM operating conditions were: acceleration voltage 15 kV, filament current 50 −100 $\mu$A, variable spot size and working distance 20 mm.

The mineralogical characterization and qualitative analysis of the bulk samples (randomly oriented) were carried out by X-ray powder diffraction (XRPD), using a SeifertGE ID 3003 diffractometer with CuK$\alpha$ radiation, Ni-filtered at 40 kV and 30 mA, whose operating conditions were: 3 −80° 2$\theta$ range, step scan 0.02°, step time 10 s. The diffraction data were analyzed using the RayfleX software package supplied by GE Inspection Technologies.

The quantitative determination of the mineralogical composition of the investigated samples was carried out by XRPD, using a Panalytical X'Pert PRO PW 3040/60 diffractometer equipped with a pyrolytic graphite analyzer crystal. Unfiltered CuK$\alpha$ radiation (40 kV, 30 mA) in the range 3 −70° 2$\theta$ was used with the following operating conditions: step scan 0.02° 2$\theta$, step time 30 s, divergence slit 0.5 mm, receiving slit 0.1 mm and anti-scatter slit 0.5°. Corundum (20 wt%) was added to the samples as an internal standard. Qantitative analysis was performed using the combined Rietveld and Reference Intensity Ratio (RIR) methods (Bish and Post, 1993; Gualtieri et al., 1996). The phase analysis was refined using X'pert HighScore Plus software, version 4.9, using the goodness of fit $\chi^2$, the profile residual $R_p$ and the weighted profile residual $R_{wp}$ as figures of merit to assess the quality of the refinement.

The error was estimated to be in the range of ±0.7 wt%. The accuracy of the refinement procedure was assessed using the profile residual $R_p$ and the weighted profile residual $R_{wp}$ as figures of merit (Larson and Von Dreele, 2004).

## 4. Results

### 4.1. Granulometric analysis

The results of the granulometric analysis, based on the Udden-Wentworth scale (Udden, 1914; Wentworth, 1922), are reported in Fig. 5. The finest clay grains found in our samples are less than 1/256 mm (3.9 $\mu$m) in size, and belong to the silt class, which is characterized by grain sizes ranging from 1/256 mm up to 1/16 mm (3.9 −62.5 $\mu$m). Silt is essentially composed of fine particles of quartz and amorphous

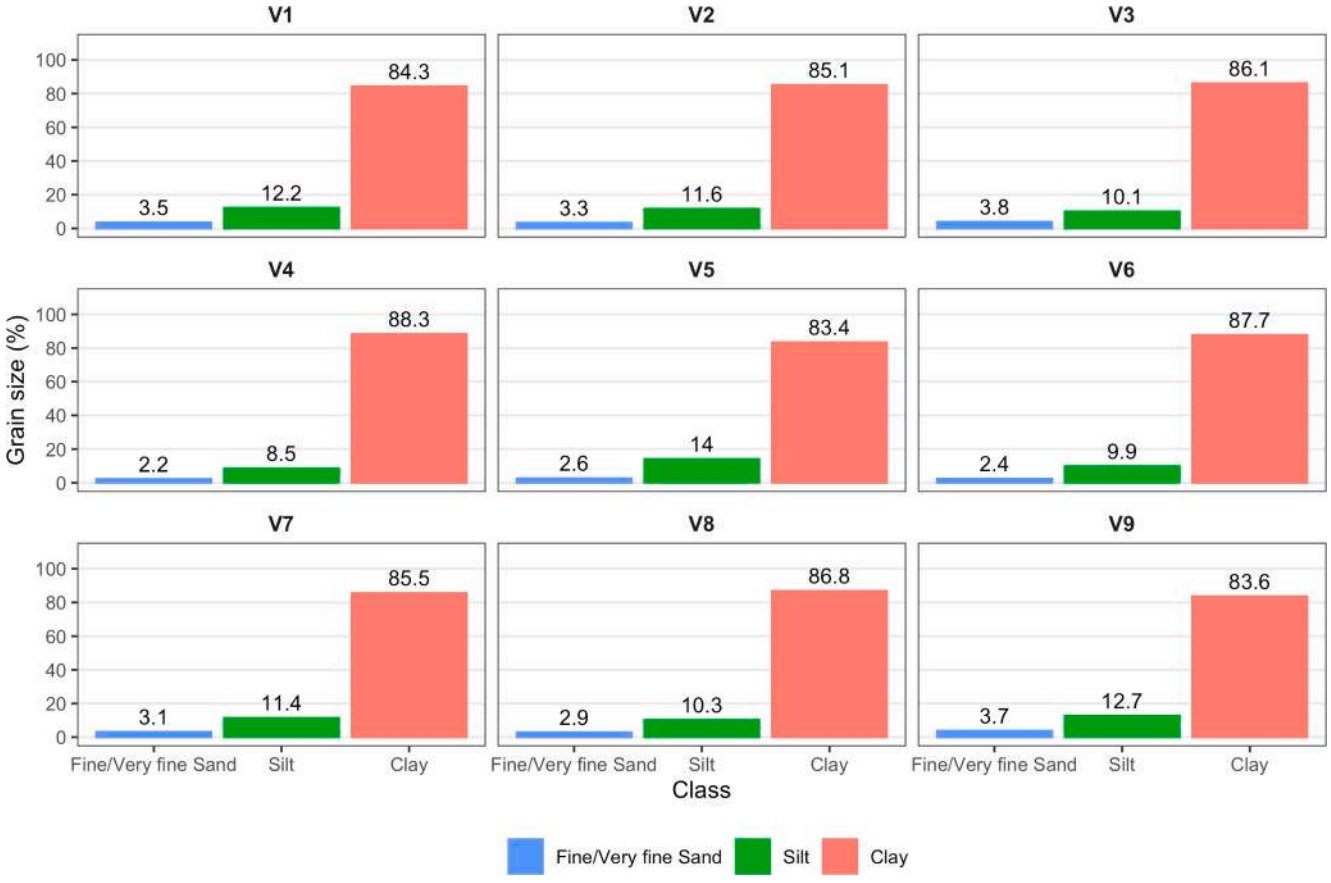


**Fig. 5.** Granulometric composition of the sediments of the MVs, in wt%. Grain size ranges are based on the Udden-Wentworth scale (Udden, 1914; Wentworth, 1922).

silica and by its nature has low plasticity and is not very permeable to percolating water. Consequently, and unlike clay, if a mud is composed mainly of silt, during the maturation process in contact with thermal water it will not absorb sufficient amounts of the active components contained in the water and therefore the therapeutic properties of the final mud will be insufficient.

The MV samples analyzed here show an excellent granulometric homogeneity, where the largest fraction is represented by clay, with a weight percentage ranging between 83.6 and 88.3 wt%, followed by the silty fraction with 8.5 −14 wt% and by the sandy fraction with a weight percentage of only 2.2 −3.8 wt% (Fig. 5). The sandy fraction is mostly composed by fine and ultrafine grains, with grain sizes between 1/16 and 1/4 mm (62.5 −250 $\mu$m) (Udden, 1914; Wentworth, 1922). Therefore, according to Shepard's classification (Shepard, 1954), all the muds considered here can be classified as true clays (Fig. 6). The strong overlap of the data points in the Figure confirms the granulometric homogeneity of the samples from the nine MVs.

According to the granulometric analysis it can thus be concluded that the naturally matured thermal muds analyzed in this study, due to their specific mineralogical composition and in particular to the predominance of clay over silt, can be effectively used in therapeutic treatments. Given the very small amount of sand contained in these muds, their application to the skin should not cause irritation due to the friction generated by rubbing.

It is worth noting that these muds may contain some potentially toxic elements (such as As, Cd, Hg, Ni and Cr) that are naturally present in the rocks that compose the upper part of the Earth's crust and end up in the clay fraction of the mud. Because of the high reactivity of the mud due to its fine grain size, these harmful components can be absorbed during the thermal treatments (Mascolo et al., 1999; Abdel-Fattah and Pingitore, 2009; Díaz Rizo et al., 2017). In fact, when the thermal mud dries on the skin, the generated heat increases blood circulation and transpiration, causing an intense local vasodilatation that promotes the elimination of toxins through the skin's excretory system and, at the same time, facilitates the absorption of the substances contained in the thermal mud. Therefore, while a fine grain size is beneficial to promote cation exchange between the organic and inorganic active components and the skin, it can also have the negative effect of facilitating the introduction of harmful components present in the mud into the organism.

### 4.2. *Geochemistry of liquid and solid fractions*

The results of the physico-chemical analysis of the liquid samples taken from the nine MVs are shown in Tables 2,3. The aqueous samples have high concentrations of $Cl^-$ and $Na^+$ ions, which gives to these geothermal fluids a typical sodium chloride composition. Another significant presence is that of hydrogen carbonate ion $HCO_3^-$, along with $Ca^{2+}$ and $Mg^{2+}$ ions. Nitrates, nitrites, and fluorides are present in very low concentrations, and also the sulfate ion $SO_4^{2-}$ is present at a fairly constant low concentration (Table 2).

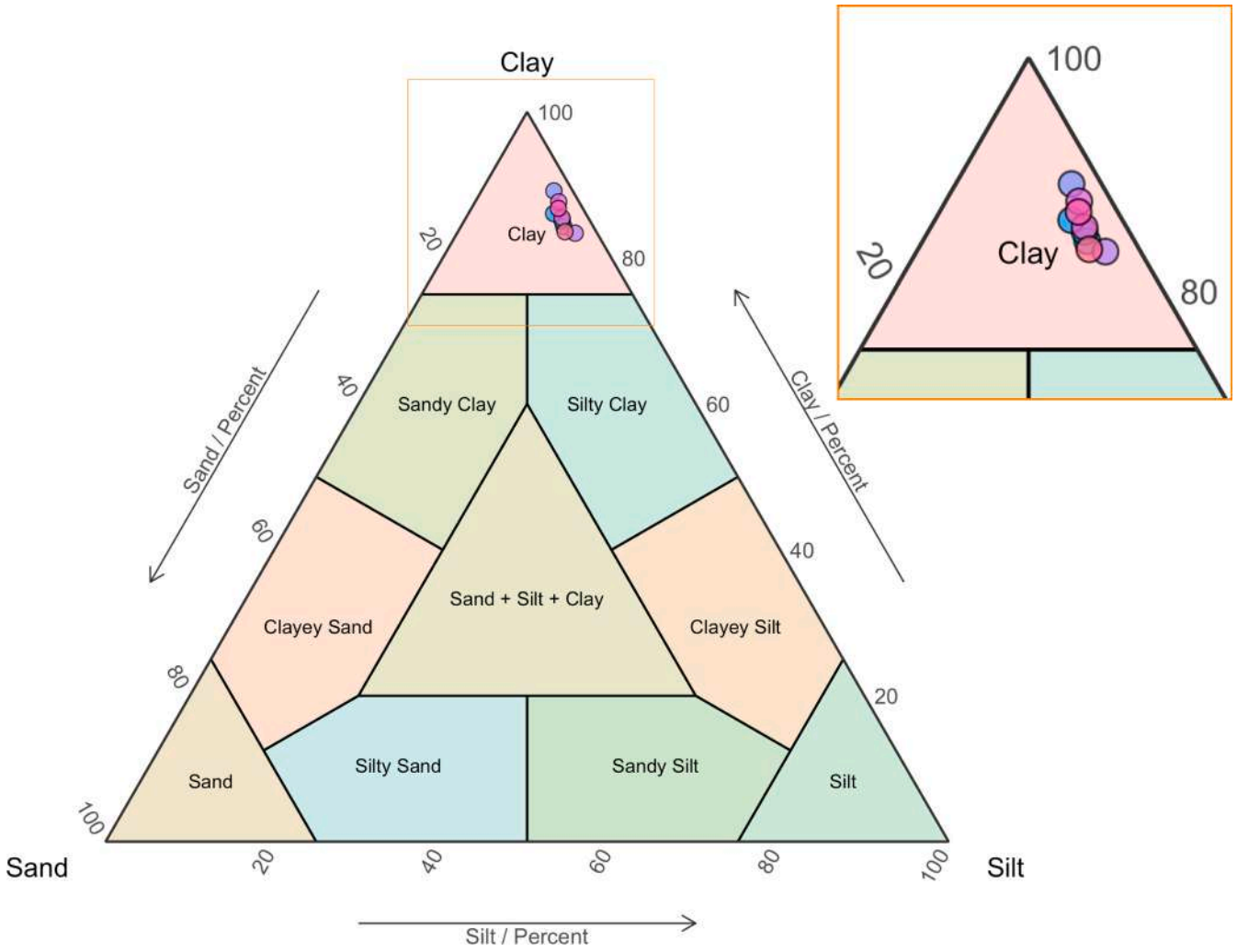


**Fig. 6.** Shepard sediment classification diagram. The dots show the resulting classification of the muds sampled from the 9 MVs. The homogeneity of the samples from the 9 MVs is visually apparent by the strong overlap of the data points.

**Table 2**
Main physico-chemical parameters of the water sampled from the MVs.

| Parameter | Unit | V1 | V2 | V3 | V4 | V5 | V6 | V7 | V8 | V9 |
|---|---|---|---|---|---|---|---|---|---|---|
| T | °C | 31.6 | 30.2 | 32.5 | 31.2 | 31.6 | 42.7 | 30.4 | 31.1 | 32.8 |
| pH | | 8.22 | 8.35 | 7.93 | 8.21 | 7.10 | 9.07 | 7.74 | 7.65 | 7.48 |
| EC | μS/cm | 61.55 | 61.71 | 54.84 | 37.62 | 53.55 | 72.81 | 38.32 | 30.47 | 51.67 |
| Eh | V | 75.23 | 98.13 | 62.36 | 77.25 | 86.52 | 121.20 | 54.30 | 46.26 | 85.05 |
| $CO_2$ | $cm^3/l$ | 19 | 24 | 31 | 29 | 16 | 27 | 18 | 20 | 28 |
| $H_2S$ | mg/l | 0.128 | 0.125 | 0.201 | 0.154 | 0.183 | 0.172 | 0.133 | 0.162 | 0.136 |
| N | mg/l | 52 | 61 | 73 | 58 | 70 | 65 | 59 | 63 | 70 |
| $Cl^-$ | mg/l | 22553 | 25874 | 18795 | 21020 | 23512 | 32124 | 16541 | 12473 | 21995 |
| $Br^-$ | mg/l | 52 | 48 | 39 | 51 | 43 | 57 | 74 | 56 | 45 |
| $I^-$ | mg/l | 39 | 44 | 38 | 54 | 56 | 47 | 56 | 41 | 50 |
| $F^-$ | mg/l | 8.4 | 9.5 | 7.2 | 6.9 | 7.1 | 8.6 | 6.5 | 6.9 | 7.2 |
| $NO_2^-$ | mg/l | 0.07 | 0.03 | 0.05 | 0.02 | 0.03 | 0.03 | 0.06 | n.a. | 0.07 |
| $NO_3^-$ | mg/l | 1.18 | 0.50 | 0.27 | 0.81 | 0.96 | 1.10 | 1.32 | 0.69 | 1.25 |
| $HCO_3^-$ | mg/l | 1875 | 1423 | 1756 | 2001 | 1985 | 1692 | 1854 | 1732 | 1811 |
| $SO_4^{2-}$ | mg/l | 86 | 101 | 75 | 84 | 97 | 119 | 67 | 56 | 88 |
| $Na^+$ | mg/l | 11955 | 14989 | 12547 | 12457 | 12899 | 17202 | 9542 | 7821 | 13022 |
| $K^+$ | mg/l | 107 | 124 | 89 | 95 | 121 | 154 | 85 | 71 | 109 |
| $Ca^{2+}$ | mg/l | 351 | 447 | 315 | 348 | 355 | 478 | 255 | 210 | 328 |
| $Mg^{2+}$ | mg/l | 254 | 366 | 272 | 214 | 296 | 438 | 257 | 169 | 244 |
| $Li^+$ | mg/l | 7 | 9 | 4 | 9 | 7 | 6 | 8 | 3 | 5 |
| $Sr^{2+}$ | mg/l | 12 | 18 | 21 | 14 | 22 | 19 | 13 | 18 | 16 |
| $Ba^{2+}$ | mg/l | 9 | 12 | 8 | 15 | 10 | 14 | 9 | 11 | 13 |

**Table 3**
Concentration of major and trace elements present in the water sampled from the MVs. All values are in μg/g.

| ID | Si | Ti | V | Cr | Mn | Fe | Co | Ni | Cu | Zn | As | Mo | Ag | Cd | Sb | Tl | Pb | U |
|---|---|---|---|---|---|---|---|---|---|---|---|---|---|---|---|---|---|---|
| V1 | 77.98 | 52.72 | 81.56 | 72.36 | 537.25 | 28475.21 | 12.54 | 27.42 | 29.54 | 87.20 | 6.01 | 0.24 | 0.12 | 0.22 | 0.18 | 0.41 | 2.43 | 1.34 |
| V2 | 85.13 | 59.32 | 68.85 | 71.38 | 454.42 | 22547.45 | 10.87 | 29.15 | 25.12 | 67.22 | 6.24 | 0.38 | 0.14 | 0.27 | 0.12 | 0.29 | 9.24 | 1.54 |
| V3 | 90.72 | 43.30 | 63.21 | 58.09 | 379.24 | 18549.44 | 13.65 | 32.54 | 27.65 | 67.35 | 7.15 | 0.45 | 0.18 | 0.24 | 0.24 | 0.25 | 8.69 | 2.27 |
| V4 | 88.56 | 147.78 | 71.47 | 57.66 | 365.31 | 29874.32 | 17.24 | 34.64 | 21.21 | 69.87 | 6.65 | 0.42 | 0.17 | 0.31 | 0.16 | 0.31 | 8.24 | 2.65 |
| V5 | 79.83 | 52.65 | 71.35 | 61.57 | 418.84 | 16578.87 | 16.34 | 37.23 | 24.32 | 61.46 | 6.24 | 0.65 | 0.11 | 0.27 | 0.14 | 0.32 | 7.34 | 1.84 |
| V6 | 82.63 | 121.25 | 69.54 | 60.78 | 442.94 | 29021.94 | 11.47 | 31.74 | 16.38 | 63.98 | 6.12 | 0.47 | 0.13 | 0.29 | 0.13 | 0.29 | 7.95 | 2.73 |
| V7 | 91.70 | 138.34 | 61.62 | 68.55 | 254.54 | 32415.54 | 8.21 | 24.15 | 18.15 | 67.41 | 7.32 | 0.64 | 0.11 | 0.27 | 0.28 | 0.23 | 8.41 | 3.11 |
| V8 | 86.18 | 48.54 | 65.23 | 71.37 | 295.65 | 21241.66 | 12.54 | 31.98 | 21.22 | 62.60 | 6.23 | 0.53 | 0.18 | 0.31 | 0.17 | 0.27 | 7.54 | 2.17 |
| V9 | 78.93 | 147.27 | 66.68 | 69.68 | 318.47 | 24591.32 | 14.11 | 32.45 | 20.41 | 64.72 | 6.01 | 0.54 | 0.16 | 0.21 | 0.19 | 0.20 | 8.21 | 2.23 |

The ion content of the liquid samples is summarized in the Piper diagram of Fig. 8, from which it can be inferred that we are in the presence of a hypertonic saline environment originated by secondary volcanic phenomena.

Regarding the metals, the chemical analyses show that they are characterized by low levels of Si, Ti, V, Cr, Co, Ni, Cu and Zn, an intermediate concentration of Mn and a much higher concentration of Fe (Table 3). The distribution of metal concentrations for the nine MVs considered here is shown in Fig. 7. The black circles superimposed to the boxplots represent the measured concentrations while the red dots show the outliers relative to the overall distribution of values for each element. All concentrations are normalized to the International Atomic Energy Agency (IAEA) safety limits (Wyse et al., 2004). These limits do not include Si and Tl, therefore these two elements have been omitted from the Figure.

Fig. 7 shows that almost all data are within the safety limits, with a very limited number of exceptions related to Co, Ni, Mn and U (ranked by number of exceedances). In all cases, the safety limits are exceeded by less than 20%, making the metal content of these thermal waters generally not harmful to human health.

Regarding temperature, the water samples analyzed here can be classified as either homeothermal (between 30°C and 40°C) or hyperthermal (between 40°C and 50°C). In almost all cases, the water temperature varies in the relatively narrow homeothermic range of 30–33°C, with the sole exception of V6, which has a significantly higher value of 42.7°C and can thus be classified as hyperthermal water. The pH plays a crucial role in determining the solubility, and thus the concentration, of metal ions in a solution. The observed values of pH, EC and Eh for V6 are higher than those measured for all the other samples,

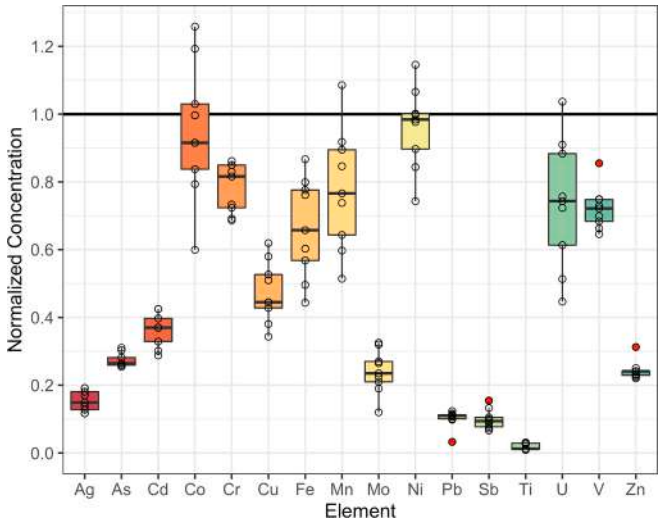


**Fig. 7.** Distribution of the measured concentrations of the elements listed in Table 3 for the 9 MVs. All concentrations are normalized to the IAEA safety limits for each element (Wyse et al., 2004). The black open circles are the actual measurements, while the red dots represent the outliers for each element.

and this difference is probably related to the much higher concentration of $Cl^-$ and $Na^+$ ions in V6 compared to all other MVs.

In summary, the water samples contain a discrete amount of sulfate and hydrogen carbonate anions as well as alkaline cations, and are

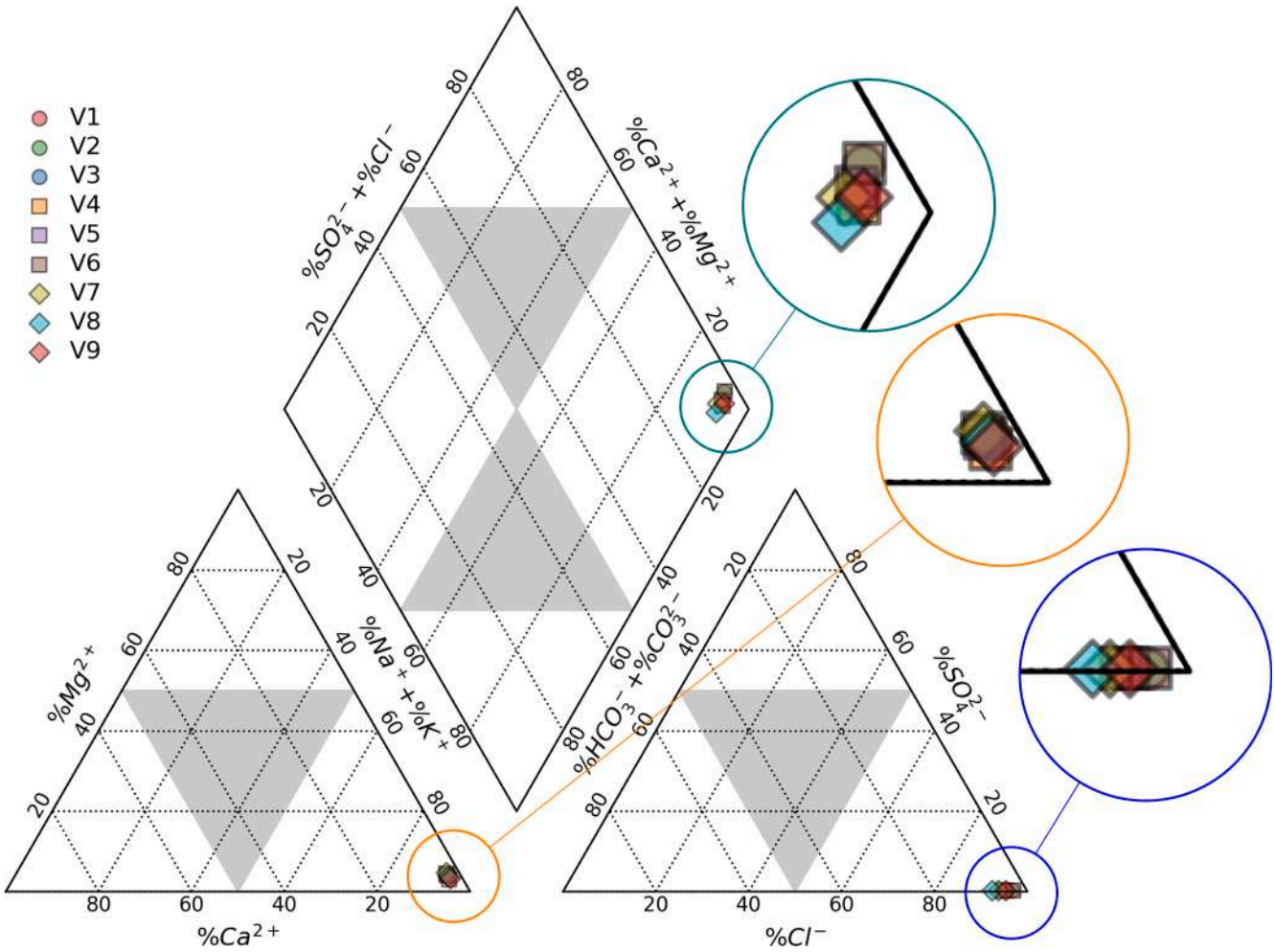


**Fig. 8.** Piper diagram of the ion content of the water samples.

characterized by a low concentration of hydrogen sulfide (Table 2). The presence of $HCO_3^-$, $Ca^{2+}$ and $Mg^{2+}$ ions allows us to further classify our aqueous samples as belonging to the bicarbonate-alkaline earth water class.

The geochemical footprint of these waters also makes them useful for treating common diseases of the respiratory system, as well as for those affecting the hepatic and gastrointestinal systems. The chemical analysis also allows us to recognize these waters as indicated for the treatment of pathologies affecting the osteoarticular and muscular system, as well as for rheumatic and vascular diseases. In contact with this characteristic water, the mud produced by the MVs acquires particular keratolytic, anti-inflammatory and immunomodulatory properties, making it particularly suitable for the treatment of affections related to the respiratory system as well as skin diseases, such as eczema, atopic dermatitis and psoriasis (Gomes et al., 2021, and references therein).

### 4.3. XRPD and SEM-EDS analysis

From a mineralogical point of view, the analyzed muds samples consist of two main crystalline components, i.e. a clay-rich fine-grained fraction and a coarser fraction consisting of minerals belonging to the groups of silicates, carbonates, sulfates, sulfides and oxides. The main minerals found in the samples, as well as their chemical formulas and symbols, are listed in Table 4. Based on the results of the quantitative XRPD of the bulk samples (Table 5), quartz, feldspar, kaolinite, chlorite, illite and smectite (likey montmorillonite, according to SEM-EDS analysis) were found in the mud samples for all the studied MVs.

**Table 4**
List of minerals cited in the text, with their chemical formulas and the corresponding name abbreviations (mainly after Warr (2021)).

| Mineral name | Formula[1] | Symbol[2] |
|---|---|---|
| Alkali feldspar group | $(K,Na)AlSi_3O_8$ | Asf |
| Apatite group | $Ca_5(PO_4)_3(OH,F,Cl)$ | |
| Barite | $Ba(SO_4)$ | Brt |
| Calcite | $CaCO_3$ | Cal |
| Chlorite group | $Mg_2Al_3(Si_3Al)\ O_{10}(OH)_8$, $(Mg,Fe)_5Al(AlSi_3O_{10})(OH)_8$ | Chl |
| Dolomite | $CaMg(CO_3)_2$ | |
| Fe-Cr oxide | | Fe-Cr ox |
| Fe-Ti oxide | | Fe-Ti ox |
| Glauberite | $Na_2Ca(SO_4)_2$ | |
| Gypsum | $Ca(SO_4)\cdot 2H_2O$ | Gp |
| Halite | NaCl | Hl |
| Hematite | $Fe_2O_3$ | Hem |
| Illite | $(K,H_3O)(Al,Mg,Fe)_2(Si,Al)_4O_{10}[(OH)_2, (H_2O)]$ | Ilt |
| Kaolinite | $Al_2Si_2O_5(OH)_4$ | Kln |
| Montmorillonite | $(Na,Ca)_{0.3}(Al,Mg)_2Si_4O_{10}(OH)_2\cdot nH_2O$ | Mnt |
| Plagioclase group | $Na(AlSi_3O_8)$, $Ca(Al_2Si_2O_8)$ | Pl |
| Pyrite | $FeS_2$ | Py |
| Quartz | $SiO_2$ | Qz |
| Sphalerite | ZnS | |

[1] According to the IMA Database of Mineral Properties (https://rruff.info/ima) and the Mineralogy Database (http://webmineral.com).
[2] Symbols used in Figs. 9–13.

**Table 5**
Quantitative XRPD analysis of the mud samples. All concentrations are in wt%.

| MV | Quartz | K-feldspar | Kaolinite | Chlorite | Illite | Montmorillonite | Dolomite | Calcite | Gypsum | Barite | Halite | Pyrite | Hematite | Amorphous |
|---|---|---|---|---|---|---|---|---|---|---|---|---|---|---|
| V1 | 26.1 | 2.8 | 20.2 | 20.4 | 4.5 | 9.2 | 0.3 | 4.8 | — | 0.5 | 3.1 | 0.9 | — | 7.2 |
| V2 | 23.6 | 3.5 | 29.3 | 3.2 | 2.3 | 4.5 | 0.2 | 0.5 | — | 0.2 | 7.0 | — | 0.3 | 25.4 |
| V3 | 25.7 | 3.7 | 28.2 | 12.4 | 4.1 | 1.1 | 0.3 | 1.0 | 0.2 | 0.2 | 1.1 | 0.2 | — | 21.8 |
| V4 | 21.0 | 4.1 | 21.5 | 1.5 | 27.6 | 1.4 | 0.2 | — | — | — | 2.4 | — | — | 20.3 |
| V5 | 27.2 | 2.6 | 22.2 | 1.9 | 26.5 | 0.9 | — | — | 1.7 | — | — | — | — | 18.1 |
| V6 | 27.2 | 8.3 | 22.2 | 7.5 | 17.9 | 5.8 | — | — | 1.4 | 0.6 | — | — | — | 9.1 |
| V7 | 22.6 | 10.9 | 18.5 | 16.6 | 14.1 | 4.5 | — | 0.7 | 2.4 | — | 0.7 | 0.3 | — | 8.7 |
| V8 | 24.5 | 17.4 | 16.5 | 15.9 | 12.6 | 3.2 | — | — | — | 0.4 | — | — | 0.2 | 9.3 |
| V9 | 23.6 | 9.2 | 18.5 | 7.1 | 24.2 | 5.2 | — | 1.8 | — | 0.9 | 1.3 | — | — | 8.2 |

The quartz content is always higher than 20 wt% and varies in a narrow interval of 21.0 −27.2 wt%, with the minimum and maximum values corresponding to the mud samples from V4 (La Bonga) and from V5 (Santa Catalina) and V6 (Clemencia), respectively (Table 1). K-feldspar varies in a much wider range, namely 2.6 −17.4 wt%, where the minimum value is found in V5 mud (Santa Catalina) and the maximum one in V8 (Cañaveral). Kaolinite ranges from 16.5 (V8) to 29.3 wt% (V2, Las Palomas), whereas a higher variability is observed for both chlorite, which ranges from 1.9 (V5) to 20.4 wt% (V1, La Laguna), and illite, which ranges from 2.3 (V2) to 27.6 wt% (V4). Montmorillonite can vary from 0.9 (V5) to 9.2 wt% (V1).

Among the minor phases identified by quantitative XRPD, small amounts of dolomite of 0.2 −0.3 wt% are detected in only four samples (from V1, V2, V3 and V4), while calcite occurs in five samples and can vary from 0.5 wt% (V2) to 4.8 wt% (V1). Barite is found in six samples and always in small percentages, from 0.2 wt% in V2 and V3 to 0.9 wt% in V9. Halite is present in six samples, ranging from 0.7 wt% (V7, Membrillal) to 7.0 wt% (V2). Pyrite occurs only in samples V1 (0.9 wt %), V3 (0.2 wt%) and V7 (0.3 wt%), while traces of hematite were observed only in samples V2 (0.3 wt%) and V8 (0.2 wt%). The amorphous fraction is also ubiquitous and varies from 7.2 wt% (V1) up to 25.4 wt% (V2).

A further estimation of the mud-forming minerals was carried out by SEM morphological observation and qualitative-semiquantitative EDS chemical analysis (Figs. 9–13). Sample V1 (Fig. 9a-c) commonly shows both kaolinite-rich (Fig. 9chlorite-rich (Fig. 9a) areas, whereas compositions attributable to montmorillonite and illite are observed to a lesser extent (Fig. 9b,c), in agreement with XRPD results. Calcite and K-feldspar grains occur randomly (Fig. 9b,c), whereas pyrite and barite occur as small disseminations in the matrix (up to about 30 $\mu$m in length, Fig. 9a,b,c).

In sample V2 halite locally forms microcrystalline coatings (Fig. 9d, f). Quartz grains (Fig. 9f) together with montmorillonite and halite-bearing areas (Fig. 9d) can also be observed. Hematite and an Fe-Ti oxide species occur as small inclusions (Fig. 9e), whereas large kaolinite-bearing fragments are also common (Fig. 9g).

Areas or scattered fragments rich in chlorite and kaolinite (Fig. 10a, b,c), with subordinate barite and halite and rare pyrite, can be observed in sample V3. Anhedral grains of K-feldspar and quartz are also detected (Fig. 10b,c). In this sample, it is also possible to observe tiny (30–40 $\mu$m) rounded aggregates, probably composed of bladed glauberite crystals (Fig. 10a,b).

The main mineralogical species in sample V4 (Fig. 11a-c) are quartz, kaolinite and illite as prevailing phyllosilicates, in agreement with the quantitative XRPD analysis. Halite is detected as microcrystalline patinas, whereas alkali feldspar occurs randomly as prismatic crystals (Fig. 11a). A sulfide, probably corresponding to an Fe-bearing sphalerite, and an Fe-Cr oxide (chromite) are also observed.

Sample V5 is quite similar to sample V4 (Fig. 11d-f), except for the presence of gypsum, barite, pyrite and a Fe-Ti oxide (the last three minerals were not identified by XRPD). A subhedral crystal of K-feldspar can be observed in Fig. 11f.

SEM-EDS micrographs of samples V6 and V7 (Fig. 12) always show the typical mineralogical association of quartz, K-feldspar, kaolinite, chlorite, illite and montmorillonite. Small amounts of gypsum and barite are also found in sample V6, together with traces of hematite (Fig. 12a-b). Gypsum, pyrite, halite and barite occur as small inclusions in sample V7 (Fig. 12c-e), although the latter mineral was not detected by XRPD.

Lastly, sample V8 shows quartz fragments, K-feldspar and hematite aggregates (Fig. 13a-b), while sample V9 is composed of a mixture of quartz, K-feldspar, kaolinite, chlorite, illite and montmorillonite (Fig. 13c-d), but grains of plagioclase, calcite and apatite are also observed (Fig. 13c).

The mineral fraction associated with the discharged fluids generally consists of clay-rich mud matrix and heterogeneous rock fragments extruded from subsurface plumbing systems of the mud volcanoes (Dimitrov, 2003; Kopf and Deyhle, 2002). The main clay mineral detected in the investigated bulk samples is kaolinite, followed by illite; samples V1 to V3 were more depleted in the latter clay species compared to samples V4 to V9. The content of chlorite and montmorillonite is more variable with respect to the other clay minerals. For the chlorite group, combined XRPD and SEM-EDS analyses point to clinochlore as the most likely phase. It is worth noting that the presence of this mineral may also represent a potential source of $Mg^{2+}$ for the waters (Babadi et al., 2021, and references therein). Furthermore, the occurrence of illite/smectite mixed layers cannot be excluded.

The qualitatively estimated low content of smectite with respect to that of illite in the muds could possibly be caused by the smectite illitization, a typical clay mineral alteration process occurring during sediment diagenesis and commonly assumed to be related to mud volcanism (Kopf and Deyhle, 2002), in analogy to what has been reported for other MVs worldwide (Williams et al., 2001; Aloisi et al., 2004; Hensen et al., 2004; You et al., 2004; Mazzini et al., 2009; Chao et al., 2011; Lavrushin et al., 2015).

With regard to the other authigenic minerals, their assemblage was found to be quite different in the nine samples analyzed, with the exception of quartz, which is predominant in all muds with a roughly constant concentration. The XRPD analysis failed to identify any polymorphic $SiO_2$ modifications other than quartz. Moreover, a detrital origin of these subordinated grains cannot be excluded.

Other minerals, such as carbonates, sulfates, sulfides and Fe-oxy-hydroxides were always found to be less than 5 wt%. Among carbonates, calcite predominates over dolomite. Gypsum, barite and glauberite are also rare and form very fine clots of anhedral to subhedral microcrystals; the same can be said for halite.

Fine crystalline pyrite (the common iron sulfide) was identified by both XRPD and qualitative SEM-EDS, while sphalerite was observed in only one sample. In two samples, i.e. V3 (Fig. 10) and V5 (Fig. 11) rounded clots of pyrite could also be attributed to framboids. As reported by Friedman et al. (1992), the deposition of pyrite, detected in many of the investigated samples, can also be a by-product of the reduction reaction of $SO_4^{2-}$ to $H_2S$ by microbial activity, according to the following equation:

$$SO_4^{2-} + 2H_2O + 2C_{org} \longrightarrow H_2S + 2HCO_3^-$$

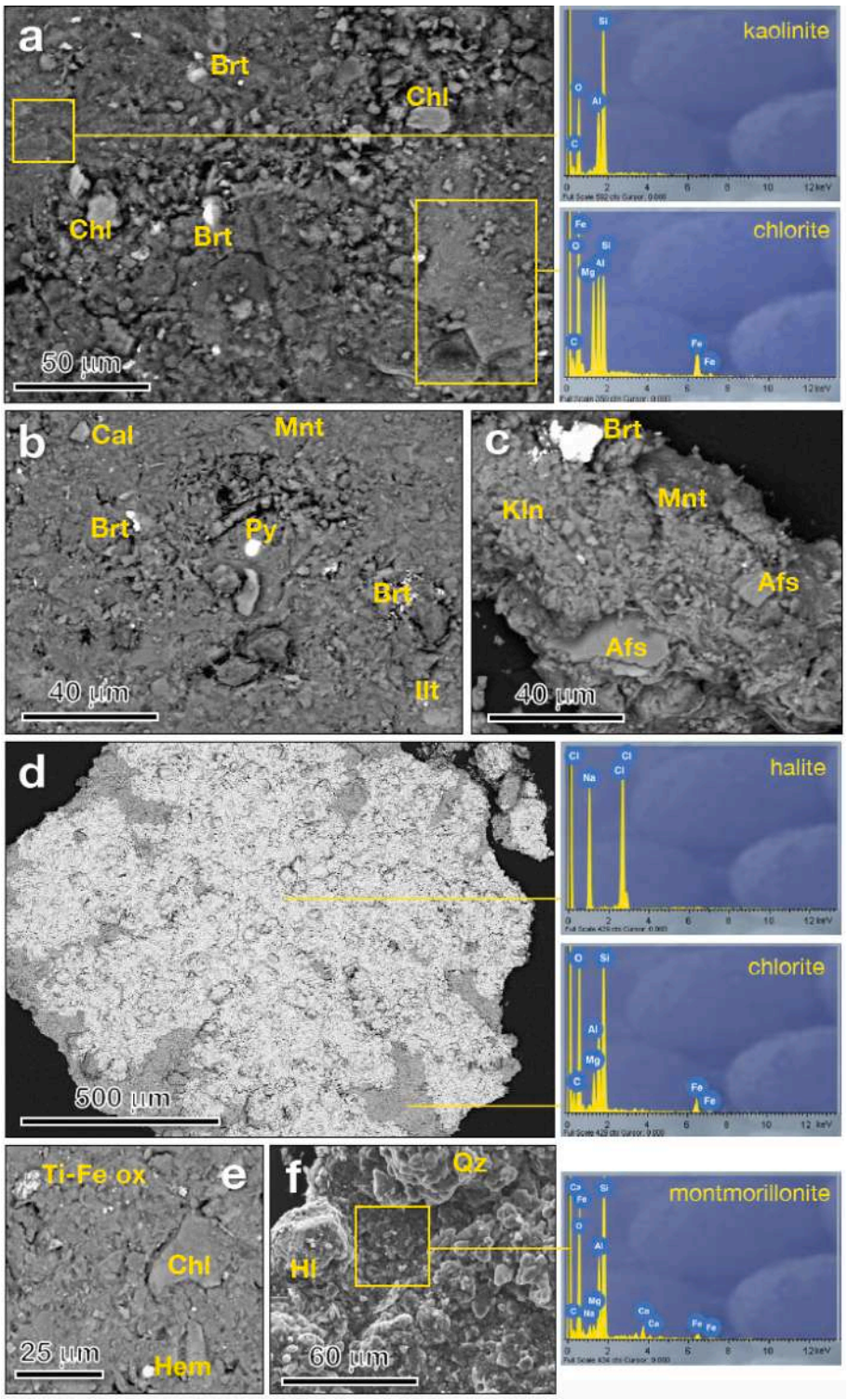


**Fig. 9.** SEM micrographs of sample V1 (a, b, c) and sample V2 (d, e, f). Abbreviations for mineral names as in Table 4. See text for a detailed description.

The smell of rotten eggs detected in the area can support the above reaction, also in relation to the presence of the $SO_4^{2-}$ found in the aqueous samples. Nevertheless, secondary $SO_4^{2-}$ could also be produced by $H_2S$ oxidation at relatively shallow depths (Babadi et al., 2021).

The clastic fraction consists mainly of feldspars (alkali feldspar prevailing over plagioclase), possibly quartz as well as sporadic spinel, clinochlore and apatite as heavy minerals and, at least to some extent, also Fe-oxy-hydroxides and pyrite.

The XRPD analysis summarized in Table 5 complements and extends with more recent samples the mineralogical results reported in Table 4 of Di Luccio et al. (2021), which was based on samples collected in the mid-2010s. Overall, we find that both studies clearly point out a mineralogical association of the muds in terms of silicates, where the main phases are quartz, kaolinite, smectite, illite and chlorite. Also, in both cases, the carbonate components are represented by calcite and dolomite.

Regarding the differences found in the two mineralogical studies, it is important to emphasize that when comparing the results of subsequent

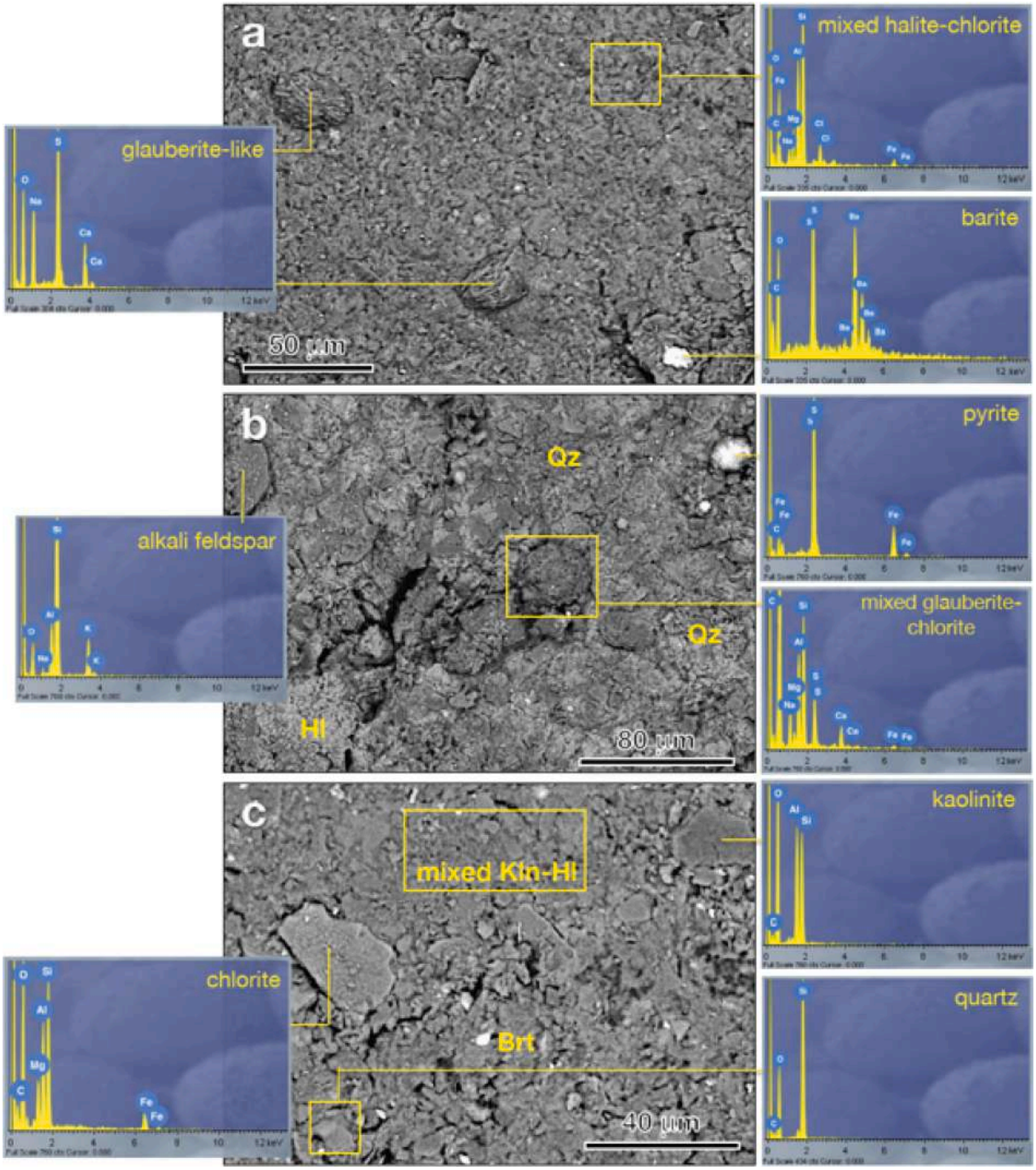


**Fig. 10.** SEM micrographs of sample V3. Abbreviations for mineral names as in Table 4. See text for a detailed description.

sampling campaigns, especially when these campaigns are carried out several years apart as reported here, significant differences between the analyses should always be expected and taken into account, even if the mud volcanoes are the same in both cases. In fact, MVs are geologically active structures, that can undergo major changes in their morphology, mineralogical composition, and geochemical behavior over the course of time. Another potential source of disagreement lies in the very extension of the mud volcanoes themselves, whose mouths can range in diameter from a few meters up to several hundred meters. Therefore, subsidence phenomena, changes in the vegetation around the mud volcano or even changes in the access paths to the MVs could have led to changes in the exact locations where sediment samples were taken in the two sampling campaigns.

## 5. Discussion and Conclusions

Mud volcanoes (MVs) are geologically dynamic structures that exhibit a wide range of mineralogical compositions, and their exploration provides valuable insights into subsurface geological processes. In particular, the mud volcanoes studied in this work provide a unique opportunity to study processes associated to a poorly understood phenomenon, in which overpressured fine-grained clay sediments are extruded to the Earth's surface from depths of up to several kilometers.

A few years ago, we carried out an extensive study of the main physical and geochemical characteristics of the same mud volcanoes along the Caribbean coast of NW Colombia (Di Luccio et al., 2021), with the aim of filling some of the existing knowledge gaps related to these

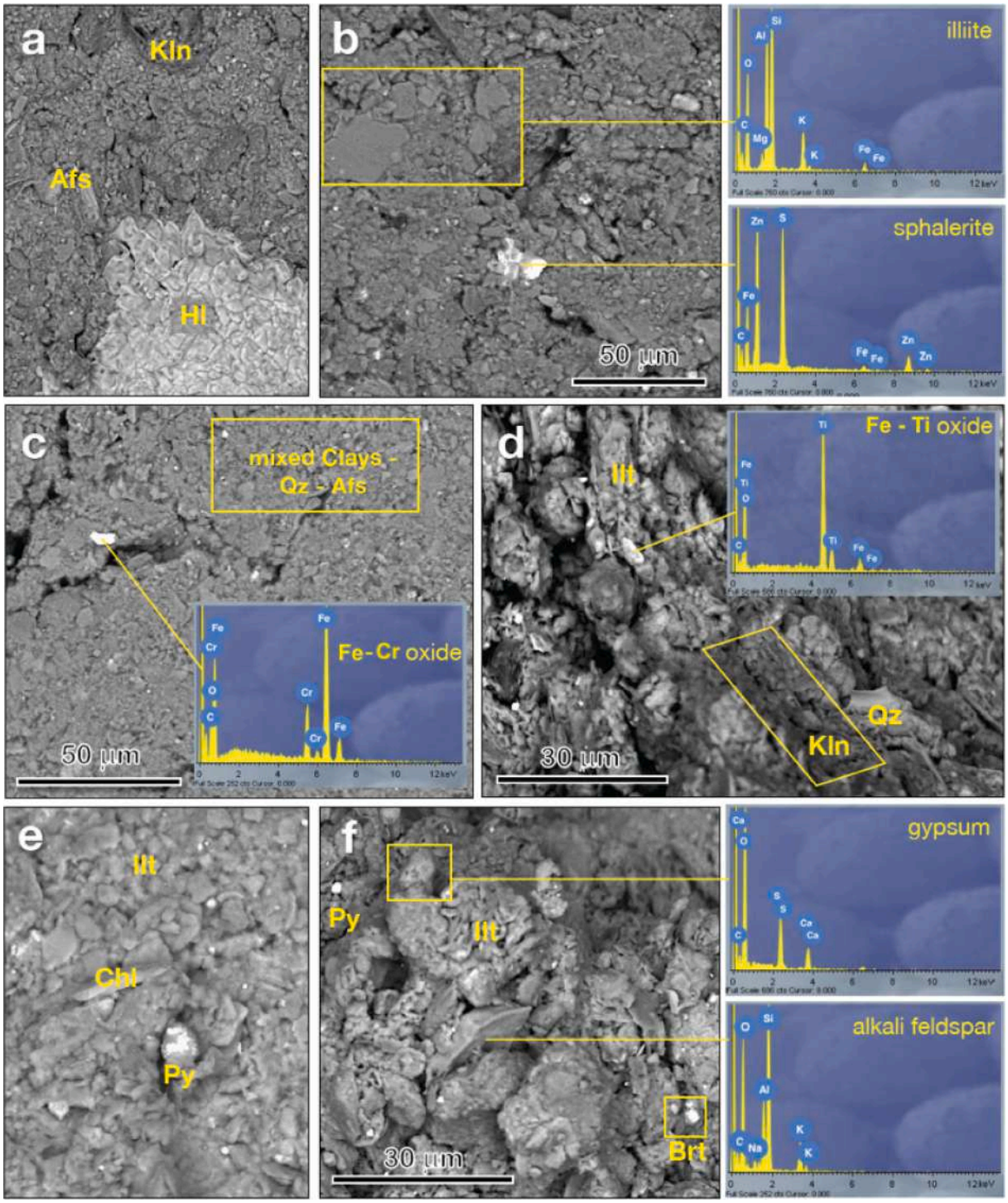


**Fig. 11.** SEM micrographs of sample V4 (a, b, c) and sample V5 ((d, e, f). Abbreviations for mineral names as in Table 4. See text for a detailed description.

geological formations.

Building on our previous work, the present study focuses on more recent samples collected in mid-2021, with the aim of gaining a more complete understanding of the evolving nature of the mud and water emissions from the MVs and to assess the potential therapeutic value of these emissions, which are of significant importance to the population living in the vicinity of these MVs. To this end, we conducted a more comprehensive analysis of the geochemical properties of both the solid and liquid fractions of the muds. In addition, a detailed mineralogical analysis was performed to determine the specific mineral composition of the muds from each MV. These analyses can provide new useful information on the geological characteristics and evolution of the studied mud volcanoes.

The granulometric analysis shows a high degree of uniformity in the particle size distribution of the muds, with clay being the predominant fraction, followed by silt and a minimal amount of sand.

The amount of silt in the mud composition (8.5 to 14 wt%) plays a crucial role in the therapeutic properties of the mud. Silt particles have low plasticity and are relatively impermeable to percolating water. If a mud consists predominantly of silt, which is composed mainly of fine quartz and amorphous silica particles, it may not effectively absorb the active components present in the thermal water during the maturation

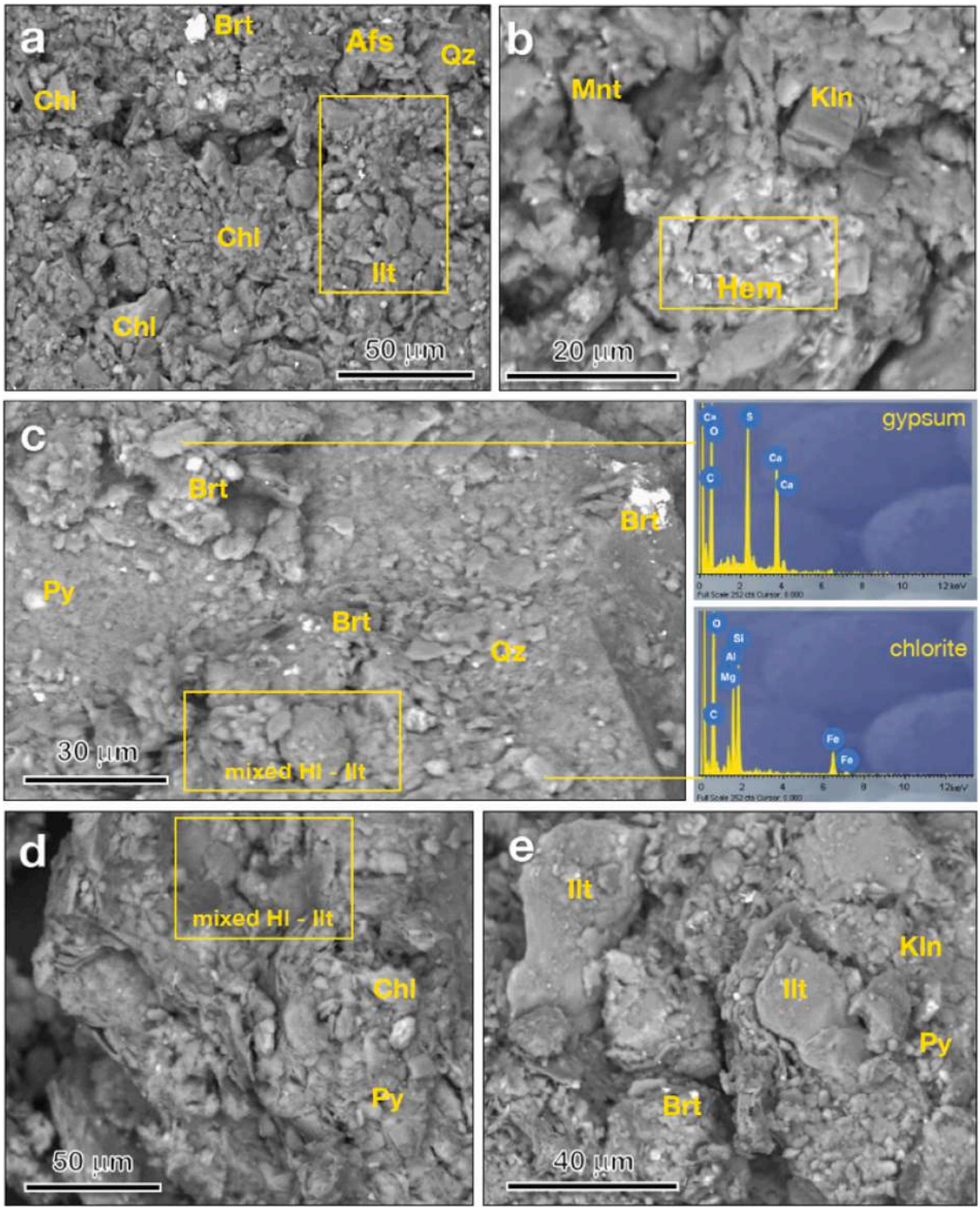


**Fig. 12.** SEM micrographs of sample V6 (a, b), and sample V7 (c, d, e). Abbreviations for mineral names as in Table 4. See text for a detailed description.

process. Consequently, the therapeutic properties of such a mud would be insufficient.

In contrast, the muds analyzed in this study exhibit a significant clay content, ranging from 83.6 wt% to 88.3 wt%. The clay fraction is known for its plasticity and permeability, allowing it to absorb and retain a wide range of active components present in the thermal water. The fine grain size of the clay particles enhances the cation exchange between the organic and inorganic components of the mud and the skin, facilitating the therapeutic effects of the mud treatments. According to Shepard's classification, these muds can therefore be classified as true clay muds. The data points in the Shepard diagram show a strong overlap, providing additional evidence for the uniformity among the samples from all nine MVs.

The low proportion of sand in the muds (2.2 −3.8 wt%) is beneficial from a therapeutic application perspective, as it reduces the potential for skin irritation caused by friction during rubbing. The fine and ultrafine grain sizes of the sandy fraction (ranging from 1/16 to 1/4 mm) contribute to the overall smoothness of the mud, enhancing its suit-

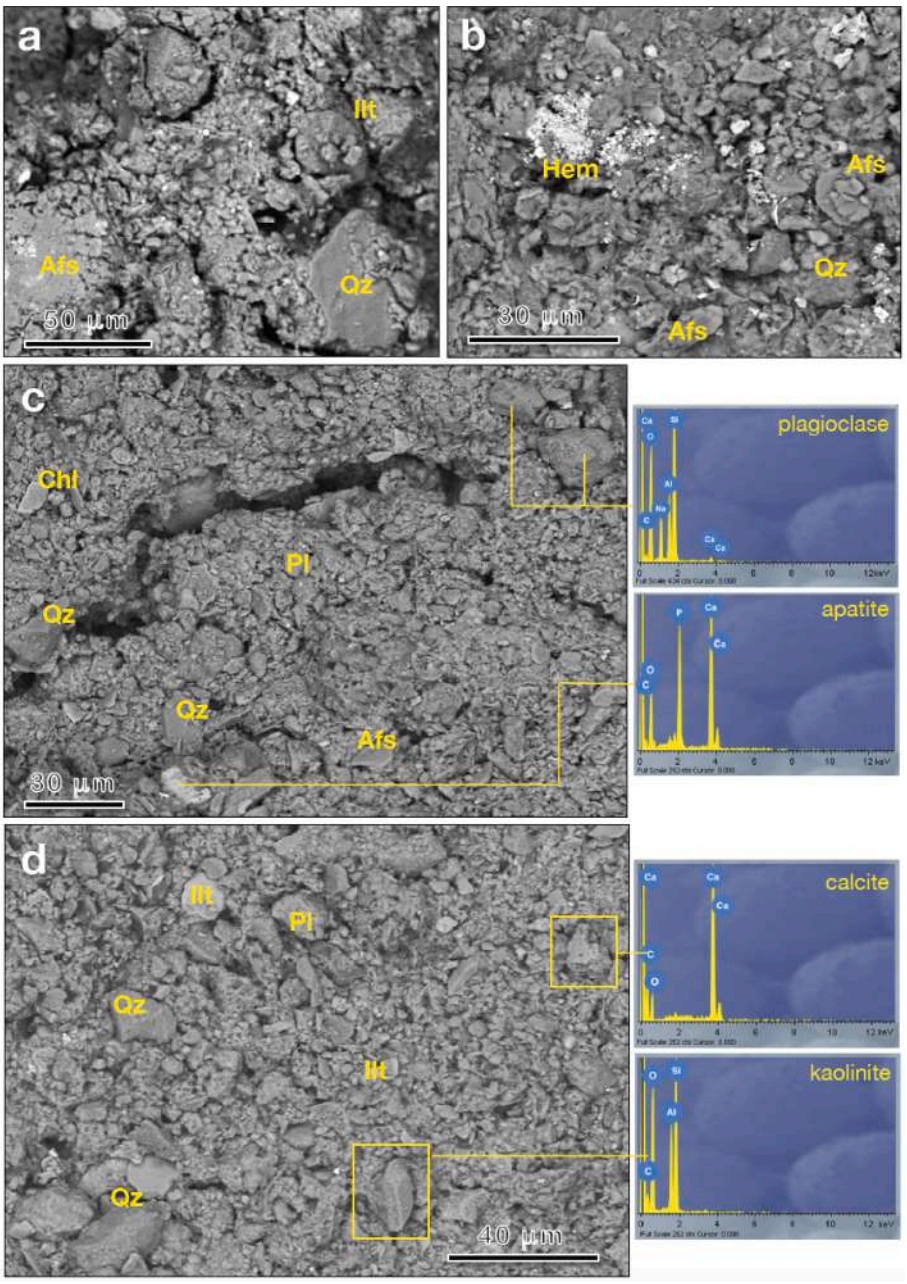


**Fig. 13.** SEM micrographs of sample V8 (a, b), and sample V9 (c, d). Abbreviations for mineral names as in Table 4. See text for a detailed description.

ability for therapeutic purposes.

It is important to note that these muds may contain potentially toxic elements, such as As, Cd, Hg, Ni, and Cr, which are naturally present in the rocks composing the Earth's crust. These elements end up in the clay fraction of the mud. The fine grain size and high reactivity of the mud increase the likelihood of absorbing such harmful components during thermal treatments. As the mud dries on the skin, the heat generated stimulates blood circulation, transpiration, and local vasodilation. This physiological response facilitates the elimination of toxins through the skin's excretory system while also enhancing the absorption of the substances contained in the mud. While the fine grain size of the mud is beneficial for promoting cation exchange between organic and inorganic components and the skin, it can also facilitate the introduction of harmful components into the organism.

The low levels of contaminants found in these muds make them safe for use by the local population. However, further research and monitoring are needed to fully assess the impact of these elements on the safety and efficacy of therapeutic treatments involving these muds.

The geochemical analysis shows a sodium chloride composition with high concentrations of $Cl^-$ and $Na^+$ ions. The presence of $HCO_3^-$, $Ca^{2+}$ and $Mg^{2+}$ ions allows us to further classify our aqueous samples as belonging to the bicarbonate-alkaline earth water class.

In terms of metal concentrations, the analyses show low levels of Si, Ti, V, Cr, Co, Ni, Cu, and Zn, intermediate levels of Mn, and significantly higher levels of Fe. Almost all metal concentrations fall well within the safety limits established by IAEA. Only a limited number of exceptions are observed, with slight exceedances of the safety limits for Co, Ni, Mn, and U. However, these exceedances are less than 20%, indicating that the metal content of these thermal waters is generally not harmful to human health.

In addition, the presence of nitrates, nitrites, and fluorides is below the critical threshold of concentration that is potentially harmful to the health of the population.

The low concentrations of nitrates, nitrites, fluorides, and sulfates

indicate a relatively pure composition of the geothermal fluids. The Piper diagram illustrates a hypertonic saline environment resulting from secondary volcanic phenomena.

The values of pH, EC, and Eh also vary among the samples, with V6 showing much higher values compared to the other MVs. This difference is probably due to the significantly higher concentrations of chloride and sodium ions in V6 compared to the other MVs.

In almost all cases, the thermal water temperature varies within the relatively narrow range of 30–33°C, and thus can be classified as homeothermal water. The only exception is the water from V6, which shows a significantly higher value of 42.7°C (hyperthermal water), associated with higher measured values of pH, EC and Eh, probably related to the much higher concentration of $Cl^-$ and $Na^+$ ions.

The thermal water temperature values recorded in the MVs studied here, which are higher than those measured in other MVs worldwide, can be explained by the tectonic setting of the region. The MVs are located on the Atlantic coast between the city of Barranquilla and the Gulf of Urabá, in an area bounded by two major faults: the Sinú Fault to the west and the Sinú-Romeral Fault System to the east (Di Luccio et al., 2021). These faults are part of a highly tectonized system that is associated with intense tectonic activity (Vernette, 1989; Briceño and Vernette, 1992; Guzmán, 2007) and may provide conduits for hot fluids to rise from depth and heat the mud at the surface. The Colombian MVs are located in a region with a high geothermal gradient, where temperature increases rapidly with depth (Quintero et al., 2019). This could also contribute to the anomalous temperature values of the water released by these volcanoes.

The mineralogical analysis has allowed to identify the composition of the solid fractions. The nine muds show a rather simple mineralogical association which, taking into account only the main minerals, is represented by quartz, phyllosilicates (kaolinite, smectite, illite and chlorite), feldspar and carbonates (dolomite, calcite), as well as a significant amorphous fraction.

Considering the main silicate phases, three different groups can be recognized: (i) kaolinite-rich (MV2 and MV3), (ii) illite-rich (MV4, MV5, MV6 and MV9), and (iii) chlorite-rich (MV1, MV7 and MV8). Among clay minerals, kaolinite and smectite (as well as talc, sepiolite and palygorskite) are the most commonly used clay minerals for medical, pharmaceutical and cosmetic applications, either as active ingredients or as excipients (Gomes and Rautureau, 2021). Illite has a geological significance (i.e “illite crystallinity index” for metamorphic facies/zone and to infer sedimentary-basin maturity for hydrocarbons), while no pharmaceutical or medical applications are known to date for chlorite (Gomes et al., 2021).

The smectite/illite ratio measured in this work is always lower than that reported in Di Luccio et al. (2021) (i.e., 0.03 −2.0 versus 1.3 −9.5). The lower amount of smectite and the higher illite content compared to the first work can be attributed to two different synchronous processes: (i) the deepening of source of the solid matrix, which may reflect a more pronounced illitization of smectite due to burial diagenesis; (ii) the localized onset of a geothermal gradient related to secondary volcanic processes (supported by the detection of pathfinder chemical components, such as $Cl^-$ and $SO_4^{2-}$), which may have promoted a “thermal baking” of smectite ending with late illitization.

Based on the results reported in this paper, it can be concluded that the characteristic geochemical composition of the waters in the study area makes them useful for treating a wide range of common diseases, including those affecting the respiratory, hepatic and gastrointestinal systems, as well as the osteoarticular, muscular, rheumatic and vascular systems.

In addition, the mud produced by the mud volcanoes in the study area has been shown to have keratolytic, anti-inflammatory and immunomodulatory properties, making it particularly suitable for the treatment of affections related to the respiratory system and of skin diseases such as eczema, atopic dermatitis and psoriasis.

Lastly, the low levels of contaminants such as potentially toxic elements, nitrates, nitrites and fluorides in these muds make them safe for use by the local population, who widely use the natural thermal pools of these mud volcanoes for pelotherapy and inexpensive recreational and wellness activities, without any limits or controls by local health or institutional authorities.

Thermal muds are unique because they are enriched with therapeutic principles during a natural maturation process. This process occurs when the mud is exposed to thermal water, sunlight and a community of thermophilic microorganisms. These microorganisms, such as cyanobacteria and microalgae, produce beneficial compounds that give the mud its therapeutic properties (Carretero, 2020; Cara et al., 2000; Fernández-González et al., 2013). In these MVs, the maturation process is completely natural, unlike what happens in spas. This natural aging process is essential for the development of the beneficial microbial community.

The microorganisms in thermal mud produce a variety of compounds with therapeutic properties, including antioxidants, anti-inflammatories, and analgesics. Thermal mud has been used to treat a variety of conditions, including arthritis, psoriasis, and eczema, and these treatments are usually safe and well tolerated.

A possible future research direction would be to implement a dedicated ground-based sensor network in conjunction with space-based observations based on the Sentinel-5P TROPOspheric Monitoring Instrument (TROPOMI) to monitor seismic activity and gaseous emissions from the mud volcanoes(Gattuso et al., 2021; Mazzini et al., 2019). This approach would provide valuable real-time information on their behavior, helping to minimize the risks of intense eruptive episodes.

Unfortunately, the current political, social and security conditions in the area make it impossible to implement such a sensor network, and the only viable option remains the monitoring of gaseous emissions by remote sensing observations. Should these conditions improve in the near future, a broader multidisciplinary approach integrating knowledge from a variety of disciplines, including geology, geophysics, geochemistry, and remote sensing, similar to that used by Castaldini et al. (2017), would undoubtedly provide further insights into the specific characteristics of the mud volcanoes under investigation. This would allow to gain a deeper understanding of the structure, composition, and dynamics of the MVs, as well as their interaction with the surrounding environment. In addition, this multidisciplinary approach would also improve our understanding of the benefits and risks associated with them. A better understanding of the factors that control mud volcano activity could help to develop more effective strategies to mitigate these risks.

## Declaration of Competing Interest

The authors declare that they have no known competing financial interests or personal relationships that could have appeared to influence the work reported in this paper.

## Data availability

Data will be made available on request.

## Acknowledgements

The authors are grateful to several colleagues for discussions and careful critical reading of the manuscript, as well as to the anonymous reviewers whose insightful comments substantially improved the quality of the paper. The authors also wish to thank Prof. N. H. Campos Campos, the director of the Centro de Estudios en Ciencias del Mar (CECIMAR) at Caribe Universidad Nacional, for his invaluable support during the field work. One of the authors (MP) acknowledges the Short-Term Mobility program of the Italian National Research Council (CNR) for providing partial financial support for this research.

## References


Abdel-Fattah, A., Pingitore, N.E., 2009. Low levels of toxic elements in Dead Sea black mud and mud-derived cosmetic products. Environ. Geochem. Health 31 (4), 487–492.

Aguzzi, C., Sánchez-Espejo, R., Cerezo, P., Machado, J., Bonferoni, C., Rossi, S., Salcedo, I., Viseras, C., 2013. Networking and rheology of concentrated clay suspensions matured in mineral medicinal water. Int. J. Pharmaceut. 453 (2), 473–479.

Aloisi, G., Drews, M., Wallmann, K., Bohrmann, G., 2004. Fluid expulsion from the Dvurechenskii mud volcano (Black Sea): Part I. Fluid sources and relevance to Li, B, Sr, I and dissolved inorganic nitrogen cycles. Earth Planet. Sci. Lett. 225 (3), 347–363.

Aristizábal, C.O., Ferrari, A.L., Silva, C.G., 2009. Control neotectónico del diapirismo de lodo en la región de Cartagena, Colombia. Ingeniería Investigación y Desarrollo I2+ D, 8(1), 42–50.

Armijo, F., Maraver, F., Pozo, M., Carretero, M.I., Armijo, O., Fernández-Torán, M.Á., Fernández-González, M.V., Corvillo, I., 2016. Thermal behaviour of clays and clay-water mixtures for pelotherapy. Appl. Clay Sci. 126, 50–56.

Atencio, C.H., Mendoza, C.D., 2018. Assessment geological, geotechnical and environmental phenomena of mud volcano in the Colombian Caribbean Coast. Scientia et technica 23 (1), 104–111.

Babadi, M.F., Mehrabi, B., Tassi, F., Cabassi, J., Pecchioni, E., Shakeri, A., Vaselli, O., 2021. Geochemistry of fluids discharged from mud volcanoes in SE Caspian Sea (Gorgan Plain, Iran). Int. Geol. Rev. 63 (4), 437–452.

Baloglanov, E.E., Abbasov, O.R., Akhundov, R.V., 2018. Mud volcanoes of the world: Classifications, activities and environmental hazard (informational-analytical review). Eur. J. Nat. History 5, 12–26.

Bish, D.L., Post, J.E., 1993. Quantitative mineralogical analysis using the Rietveld full-pattern fitting method. Am. Mineral. 78 (9–10), 932–940.

Briceño, L.A., Vernette, G., 1992. Manifestaciones del diapirismo arcilloso en el margen colombiano del Caribe. Earth Sci. Res. J. 1, 21–30.

Brown, K., Westbrook, G.K., 1988. Mud diapirism and subcretion in the Barbados Ridge accretionary complex: the role of fluids in accretionary processes. Tectonics 7 (3), 613–640.

Burt, B., 1949. Décisions prises au cours de la session 1949. In: In Proceedings of the IVe Conférence Scientifique Internationale de Dax, pp. 13–16.

Cara, S., Carcangiu, G., Padalino, G., Palomba, M., Tamanini, M., 2000. The bentonites in pelotherapy: thermal properties of clay pastes from Sardinia (Italy). Appl. Clay Sci. 16 (1–2), 125–132.

Carretero, M.I., Gomes, C.S.F., Tateo, F., 2006. Clays and Human Health. In: Bergaya, F., Theng, B.K., Lagaly, G. (Eds.), Handbook of Clay Science, volume 1 of Developments in Clay Science, chapter 11.5. Elsevier, pp. 717–741.

Carretero, M.I., Lagaly, G., 2007. Clays and health: An introduction. Appl. Clay Sci. 36 (1), 1–3.

Carretero, M.I., 2002. Clay minerals and their beneficial effects upon human health. A review. Applied Clay Science 21 (3–4), 155–163.

Carretero, M.I., 2020. Clays in pelotherapy. A review. Part I: Mineralogy, chemistry, physical and physicochemical properties. Appl. Clay Sci. 189, 105526.

Carvajal, J.H., Mendivelso, D., 2011. Catálogo de volcanes de lodo Caribe Central Colombiano. Technical report, Instituto Colombiano De Geología Y Minería INGEOMINAS.

Carvajal, J.H., Mendivelso, D., Obando, G., Forero, H., Gómez, J.F., Vásquez, L., Mora, H., Cárdenas, R., Castiblanco, C.R., Franco, J.V., Ruge, G., Pinzón, L., Prada, M.Á., Imbachi, O., 2011. Características del volcanismo de lodo del Caribe central colombiano. Technical report, Instituto Colombiano De Geología Y Minería INGEOMINAS.

Castaldini, D., Conventi, M., Coratza, P., Tosatti, G., editors, 2017. Studi interdisciplinari in Scienze della Terra per la fruizione in sicurezza della Riserva Naturale delle Salse di Nirano, volume 148 Supplemento, Modena, Italia, 2017. ISBN 0365-7027.

F. Cediel, R.P. Shaw, and C. Cáceres. Tectonic Assembly of the Northern Andean Block. In C. Bartolini, R.T. Buffer, and J. Blickwede, editors, The Circum-Gulf of Mexico and the Caribbean: Hydrocarbon Habitats, Basin Formation and Plate Tectonics, volume 79, pages 815–848. American Association of Petroleum Geologists, 2003.

Chao, H.-C., You, C.-F., Wang, B.-S., Chung, C.-H., Huang, K.-F., 2011. Boron isotopic composition of mud volcano fluids: Implications for fluid migration in shallow subduction zones. Earth Planet. Sci. Lett. 305 (1), 32–44.

Conti, S., Fontana, D., Lucente, C.C., Pini, G.A., 2014. Relationships between seep-carbonates, mud volcanism and basin geometry in the Late Miocene of the northern Apennines of Italy: the Montardone mélange). Int. J. Earth Sci. 103 (1), 281–295.

Danzi, M., 2017. Le terme in Europa tra letteratura e medicina. Quaderns d'Italià 22, 43–56.

Deville, E., Battani, A., Griboulard, R., Guerlais, S.H., Lallemant, S., Mascle, A., Prizhofer, A., Schmitz, J., 2003. Processes of mud volcanism in the Barbados-Trinidad compressional system: new structural, thermal and geochemical data. In Proceedings of AAPG Annual Meeting, Salt Lake City, UT, USA, 11–14 May 2003.

Di Luccio, D., Banda Guerra, I.M., Correa Valero, L.E., Morales Giraldo, D.F., Maggi, S., Palmisano, M., 2021. Physical and geochemical characteristics of land mud volcanoes along Colombia's Caribbean coast and their societal impacts. Science of The Total Environment 759, 144225.

Dill, H.G., Kaufhold, S., 2018. The Totumo mud volcano and its near-shore marine sedimentological setting (North Colombia)—From sedimentary volcanism to epithermal mineralization. Sed. Geol. 366, 14–31.

Dill, H.G., Balaban, S.-I., Buzatu, A., Bornemann, A., Techmer, A., 2022. The Quaternary volcanogenic landscape and volcaniclastic sediments of the Netherlands Antilles: markers for an in-active volcanic arc. Int. J. Earth Sci. 111 (1), 149–187.

Dimitrov, L.I., 2002. Mud volcanoes — The most important pathway for degassing deeply buried sediments. Earth Sci. Rev. 59 (1–4), 49–76.

Dimitrov, L.I., 2003. Mud volcanoes – A significant source of atmospheric methane. Geo-Mar. Lett. 23 (3–4), 155–161.

Díaz Rizo, O., Suárez Muñoz, M., González Hernández, P., Gelen Rudnikas, A., D'Alessandro Rodríguez, K., Melián Rodríguez, C.M., Pérez Martín, A., Fagundo Castillo, J.R., Martínez-Villegas, N.V., 2017. Assessment of heavy metal content in peloids from some Cuban spas using X-ray fluorescence. Nucleus 61, 237–240.

Etiope, G., Feyzullayev, A., Baciu, C.L., Milkov, A.V., 2004. Methane emission from mud volcanoes in eastern Azerbaijan. Geology 32 (6), 465–468.

Fernández-González, M.V., Martín-García, J.M., Delgado, G., Párraga, J., Delgado, R., 2013. A study of the chemical, mineralogical and physicochemical properties of peloids prepared with two medicinal mineral waters from Lanjarón Spa (Granada, Spain). Appl. Clay Sci. 80, 107–116.

Friedman, G.M., Sanders, J.E., Kopaska-Merkel, D.C., 1992. Principles of sedimentary deposits: Stratigraphy and sedimentology. Macmillan Publishing Company, New York.

Galzigna, L., Lalli, A., Moretto, C., Bettero, A., 1995. Maturation of thermal controlled conditions and identification of an antiinflammatory fraction. Physikalische Medizin, Rehabilitationsmedizin, Kurortmedizin 5 (6), 196–199.

García-Delgado, H., Velandia, F., Bermúdez, M.A., Audemard, F., 2022. The present-day tectonic regimes of the Colombian Andes and the role of slab geometry in intraplate seismicity. Int. J. Earth Sci. 111 (7), 2081–2099.

Gattuso, A., Italiano, F., Capasso, G., D'Alessandro, A., Grassa, F., Pisciotta, A.F., Romano, D., 2021. The mud volcanoes at santa barbara and aragona (sicily, italy): a contribution to risk assessment. Natural Hazards and Earth System Sciences 21 (11), 3407–3419.

Gomes, C., Silva, J., 2006. Products based on clay, mud, and sand with interest for balneotherapy. Clay Science 12 (Supplement 2), 228–232.

Gomes, C.d.S.F., Silva, J.B.P., 2007. Minerals and clay minerals in medical geology. Appl. Clay Sci. 36 (1–3), 4–21.

Gomes, C., Carretero, M.I., Pozo, M., Maraver, F., Cantista, P., Armijo, F., Legido, J.L., Teixeira, F., Rautureau, M., Delgado, R., 2013. Peloids and pelotherapy: Historical evolution, classification and glossary. Appl. Clay Sci. 75, 28–38.

Gomes, C., Rautureau, M. (Eds.), 2021. Minerals latu sensu and Human Health. Springer, Switzerland.

C. Gomes. Mineral-based products for applications in balneotherapy: an interesting field for research, development and innovation. In Proceedings of the XIX Reunión Científica de la Sociedad Española de Arcillas, volume 89, page 90, Salamanca, España, 2005.

Gualtieri, A., Norby, P., Hanson, J., Hriljac, J., 1996. Rietveld refinement using synchrotron X-ray powder diffraction data collected in transmission geometry using an imaging-plate detector: application to standard m-ZrO2. J. Appl. Crystallogr. 29 (6), 707–713.

Guzmán, G., 2007. Stratigraphy and sedimentary environment and implications in the plato basin and the San Jacinto Belt northwestern Colombia. PhD thesis. University of Liège.

Hensen, C., Wallmann, K., Schmidt, M., Ranero, C.R., Suess, E., 2004. Fluid expulsion related to mud extrusion off costa rica—a window to the subducting slab. Geology 32 (3), 201–204.

Higgins, G.E., Saunders, J.B., 1974. Mud volcanoes — their nature and origin: contribution to the geology and paleobiology of the caribbean and adjacent areas. Verhandlungen der Naturforschenden Gesellschaft in Basel 84, 101–152.

Hosein, R., Haque, S., Beckles, D.M., 2014. Mud volcanoes of Trinidad as astrobiological analogs for Martian environments. Life 4 (4), 566–585.

Jobstraibizer, P., 1999. Definizione mineralogica e chimica del fango termali e per trattamenti dermatologici e cosmetici. Montecatini Terme. Mineralogica et Petrographica Acta 42, 317–327.

Kopf, A., Deyhle, A., 2002. Back to the roots: boron geochemistry of mud volcanoes and its implications for mobilization depth and global B cycling. Chem. Geol. 192 (3–4), 195–210.

Kopf, A.J., 2002. Significance of mud volcanism. Rev. Geophys. 40 (2), 1–52.

Krumbein, W.C., 1934. Size frequency distributions of sediments. J. Sediment. Res. 4 (2), 65–77.

Larson, A.C., Von Dreele, R.B., 2004. General structure analysis system (GSAS). Technical report, Los Alamos National Laboratory Report LAUR 86–748, New Mexico, USA.

Lavrushin, V.Y., Guliev, I.S., Kikvadze, O.E., Aliev, A.A., Pokrovsky, B.G., Polyak, B.G., 2015. Waters from mud volcanoes of Azerbaijan: Isotopic-geochemical properties and generation environments. Lithol. Min. Resour. 50 (1), 1–25.

G. Lüttig. Peloid therapy in Germany - A state of the art. In Proceedings of the 3rd Symposium on Thermal Muds in Europe, 25–27 Novembre, Dax (France) (2004), pages 16–22, 2004.

Maestrelli, D., Bonini, M., Sani, F., 2019. Linking structures with the genesis and activity of mud volcanoes: examples from Emilia and Marche (Northern Apennines, Italy). Int. J. Earth Sci. 108 (5), 1683–1703.

A.M. Mantilla-Pimiento, G. Jentzsch, J. Kley, and C. Alfonso-Pava. Configuration of the Colombian Caribbean Margin: Constraints from 2D Seismic Reflection data and Potential Fields Interpretation. In S. Lallemand and F. Funiciello, editors, Subduction Zone Geodynamics, pages 247–272, Berlin, Heidelberg, 2009. Springer.

Mascolo, N., Summa, V., Tateo, F., 1999. Characterization of toxic elements in clays for human healing use. Appl. Clay Sci. 15 (5–6), 491–500.

Mazzini, A., Etiope, G., 2017. Mud volcanism: an updated review. Earth Sci. Rev. 168, 81–112.

Mazzini, A., Svensen, H., Planke, S., Guliyev, I., Akhmanov, G.G., Fallik, T., Banks, D., 2009. When mud volcanoes sleep: Insight from seep geochemistry at the Dashgil mud volcano. Azerbaijan. Marine and Petroleum Geology 26 (9), 1704–1715.
Mazzini, A., Sciarra, A., Etiope, G., Sadavarte, P., Houweling, S., Pandey, S., Husein, A., 2019. Relevant methane emission to the atmosphere from a geological gas manifestation. Scientific Reports, 11:4138/1–10.
Panzera, F., Sicali, S., Lombardo, G., Imposa, S., Gresta, S., D'Amico, S., 2016. A microtremor survey to define the subsoil structure in a mud volcanoes area: the case study of Salinelle (Mt. Etna, Italy). Environmental Earth Sciences 75 (15), 1140-13.
Photos-Jones, E., Christidis, G., Piochi, M., Keane, C., Mormone, A., Balassone, G., Perdikatsis, V., Leanord, A., 2016. Testing greco-roman medicinal minerals: The case of solfataric alum. Journal of Archaeological Science: Reports 10, 82–95.
Pozo, M., Armijo, F., Maraver, F., Zuluaga, P., Ejeda, J.M., Corvillo, I., 2019. Variations in the texture profile analysis (tpa) properties of clay/mineral-medicinal water mixtures for pelotherapy: Effect of anion type. Minerals 9 (3), 144/1–16.
Quintela, A., Terroso, D., Ferreira da Silva, E., Rocha, F., 2012. Certification and quality criteria of peloids used for therapeutic purposes. Clay Miner. 47 (4), 441–451.
Quintela, A., Terroso, D., Costa, C., Sá, H., Nunes, J.C., Rocha, F., 2015. Characterization and evaluation of hydrothermally influenced clayey sediments from Caldeiras da Ribeira Grande fumarolic field (Azores Archipelago, Portugal) used for aesthetic and pelotherapy purposes. Environmental Earth Sciences 73 (6), 2833–2842.
W. Quintero, O. Campos-Enríquez, and O. Hernández. Curie point depth, thermal gradient, and heat flow in the colombian caribbean (northwestern south america). Geothermal Energy, 7:16/1–20, 2019.
Rebelo, M., da Silva, E.F., Rocha, F., 2015. Characterization of Portuguese thermo-mineral waters to be applied in peloids maturation. Environmental Earth Sciences 73 (6), 2843–2862.
Ren, G., Ma, A., Zhang, Y., Deng, Y., Zheng, G., Zhuang, X., Zhuang, G., Fortin, D., 2018. Electron acceptors for anaerobic oxidation of methane drive microbial community structure and diversity in mud volcanoes. Environmental microbiology 20 (7), 2370–2385.
Shepard, F.P., 1954. Nomenclature Based on Sand-Silt-Clay Ratios. J. Sediment. Res. 24 (3), 151–158.
Sokol, E.V., Kokh, S.N., Kozmenko, O.A., Lavrushin, V.Y., Belogub, E.V., Khvorov, P.V., Kikvadze, O.E., 2019. Boron in an onshore mud volcanic environment: Case study from the kerch peninsula, the caucasus continental collision zone. Chem. Geol. 525, 58–81.
Sánchez-Espejo, R., Aguzzi, C., Salcedo, I., Cerezo, P., Viseras, C., 2014. Clays in complementary and alternative medicine. Mater. Technol. 29 (sup3), B78–B81.
Tateo, F., Summa, V., 2007. Element mobility in clays for healing use. Appl. Clay Sci. 36 (1–3), 64–76.
Udden, J.A., 1914. Mechanical Composition of Clastic Sediments. GSA Bulletin 25 (1), 655–744.
Veniale, F., Barberis, E., Carcangiu, G., Morandi, N., Setti, M., Tamanini, M., Tessier, D., 2004. Formulation of muds for pelotherapy: effects of maturation by different mineral waters. Appl. Clay Sci. 25 (3–4), 135–148.
Veniale, F., Bettero, A., Jobstraibizer, P.G., Setti, M., 2007. Thermal muds: Perspectives of innovations. Appl. Clay Sci. 36 (1–3), 141–147.
Vernette, G., Mauffret, A., Bobier, C., Briceno, L., Gayet, J., 1992. Mud diapirism, fan sedimentation and strike-slip faulting. Caribbean Colombian Margin. Tectonophysics 202 (2), 335–349.
Vernette, G., 1989. Examples of diapiric control on shelf topography and sedimentation patterns on the Colombian Caribbean continental shelf. J. S. Am. Earth Sci. 2 (4), 391–400.
Vinnels, J.S., Butler, R.W.H., McCaffrey, W.D., Paton, D.A., 2010. Depositional processes across the Sinú Accretionary Prism, offshore Colombia. Mar. Pet. Geol. 27 (4), 794–809.
Warr, L.N., 2021. IMA–CNMNC approved mineral symbols. Mineral. Mag. 85 (3), 291–320.
Wentworth, C.K., 1922. A Scale of Grade and Class Terms for Clastic Sediments. J. Geol. 30 (5), 377–392.
Williams, L.B., Hervig, R.L., Holloway, J.R., Hutcheon, I., 2001. Boron isotope geochemistry during diagenesis. Part I. Experimental determination of fractionation during illitization of smectite. Geochim. Cosmochim. Acta 65 (11), 1769–1782.
Wyse, E.J., Coquery, M., Azemard, S., de Mora, S.J., 2004. Characterisation of trace elements and methylmercury in an estuarine sediment reference material, IAEA-405. J. Environ. Monit. 6 (1), 48–57.
You, C.-F., Gieskes, J.M., Lee, T., Yui, T.-F., Chen, H.-W., 2004. Geochemistry of mud volcano fluids in the Taiwan accretionary prism. Appl. Geochem. 19 (5), 695–707.